Journal of Medicinal Chemistry

Article

Synthesis, Structure-Activity Relationships and In Vivo Efficacy of the Novel Potent and Selective Anaplastic Lymphoma Kinase (ALK) Inhibitor LDK378 Currently In Phase 1 and 2 Clinical Trials

Tom H. Marsilje, Wei Pei, Bei Chen, Wenshuo Lu, Tetsuo Uno, Yunho Jin, Tao Jiang, Sungjoon Kim, Nanxin Li, Markus Warmuth, Yelena Sarkisova, Fangxian Sun, Auzon Steffy, AnneMarie C. Pferdekamper, Sean B Joseph, Young Kim, Tove Tuntland, Xiaoming Cui, Nathanael S Gray, Ruo Steensma, Yongqin Wan, Jiqing Jiang, Jie Li, Greg Chopiuck, W. Perry Gordon, Allen G Li, Wendy Richmond, Johathan Chang, Todd Groessl, You-Qun He, Bo Liu, Andrew Phimister, Alex Aycinena, Badry Bursulaya, Christian Lee, Donald S Karanewsky, H Martin Seidel, Jennifer L Harris, and Pierre-Yves Michellys

J. Med. Chem., **Just Accepted Manuscript** • DOI: 10.1021/jm400402q • Publication Date (Web): 06 Jun 2013

Journal of Medicinal Chemistry is published by the American Chemical Society. 1155 Sixteenth Street N.W., Washington, DC 20036

	Jiang, Jiqing; Genomics Institute of the Novartis Research Foundation, Li, Jie; Genomics Institute of the Novartis Research Foundation, Medicinal Chemistry Chopiuck, Greg; Investors Group, Gordon, W.; Genomics Institute of the Novartis Research Foundation, Li, Allen; PhaseRx Inc., Richmond, Wendy; Genomics Institute of the Novartis Research Foundation, Chang, Johathan; Genomics Institute of the Novartis Research Foundation, Groessl, Todd; Genomics Institute of the Novartis Research Foundation, He, You-Qun; Genomics Institute of the Novartis Research Foundation, Liu, Bo; Genomics Institute of the Novartis Research Foundation, Phimister, Andrew; Novartis Vaccines and Diagnostics,, Aycinena, Alex; Novartis Vaccines and Diagnostics,, Bursulaya, Badry; Genomics Institute of the Novartis Research Foundation, Lee, Christian; Genomics Institute of the Novartis Research Foundation, Protein Science Karanewsky, Donald; Senomyx Inc., Seidel, H; Genomics Institute of the Novartis Research Foundation, Harris, Jennifer; Genomics Institute of the Novartis Research Foundation, Michellys, Pierre-Yves; Genomics Institute of the Novartis Research Foundation, Medicinal chemistry

Synthesis, Structure-Activity Relationships and *In Vivo* Efficacy of the Novel Potent and Selective Anaplastic Lymphoma Kinase (ALK) Inhibitor 5-chloro-N2-(2-isopropoxy-5-methyl-4-(piperidin-4-yl)phenyl)-N4-(2-(isopropylsulfonyl)phenyl)pyrimidine-2,4-diamine (LDK378) Currently In Phase 1 and 2 Clinical Trials

*Thomas H. Marsilje, Wei Pei, Bei Chen, Wenshuo Lu, Tetsuo Uno, Yunho Jin, Tao Jiang, Sungjoon Kim, Nanxin Li, Markus Warmuth, Yelena Sarkisova, Frank Sun, Auzon Steffy, AnneMarie C. Pferdekamper, Allen G. Li, Sean B. Joseph, Young Kim, Bo Liu, Tove Tuntland, Xiaoming Cui, Nathanael S Gray, Ruo Steensma, Yongqin Wan, Jiqing Jiang, Greg Chopiuck, Jie Li, W. Perry Gordon, Wendy Richmond, Kevin Johnson, Jonathan Chang, Todd Groessl, You-Qun He, Andrew Phimister, Alex Aycinena, Christian C. Lee, Badry Bursulaya, Donald S. Karanewsky, H. Martin Seidel, Jennifer L. Harris, Pierre-Yves Michellys.**

KEYWORDS. ALK, ALKi, SAR, ALCL, NSCLC, Karpas299, NCI-H2228, kinase.

ABSTRACT. The synthesis, pre-clinical profile and *in vivo* efficacy in rat xenograft models of the novel and selective anaplastic lymphoma kinase inhibitor **15b** (LDK378) is described. In this initial report,

preliminary structure-activity relationships (SAR) are described as well as the rational design strategy employed to overcome the development deficiencies of the first generation ALK inhibitor **4** (TAE684). Compound **15b** is currently in Phase 1 and 2 clinical trials with substantial antitumor activity being observed in ALK-positive cancer patients.

Introduction

Anaplastic lymphoma kinase (ALK) is a receptor tyrosine kinase of the insulin receptor superfamily. Expression of ALK in normal human tissues is only found in a subset of neural cells.[1] However, altered expression and hyperactivation of ALK as a consequence of translocations or point mutations has been demonstrated to be an essential oncogenic lesion in a number of cancers.[2-4] To date, no essential role has been found for ALK in mammals. Mice deficient in ALK have normal development and display an anti-depressive phenotype with enhanced performance in hippocampus-dependent tasks, potentially due to increased hippocampal progenitor cells.[5]

Deregulation of ALK was first identified in anaplastic large cell lymphoma (ALCL), where the tyrosine kinase domain is fused to nucleophosmin (NPM), a product of recurrent t(2;5)(p23;q35) chromosomal translocation.[6] Subsequently, chromosomal rearrangements resulting in ALK fused to various partner genes have been found in nearly 70% of ALCL, 40-60% of inflammatory myofibroblastic tumors (IMT),[7] a few dozen cases of diffuse large B-cell lymphoma (DLBCL), and, most recently, in 2-7% of non-small cell lung cancer (NSCLC).[8-10] Among fusion partner genes identified to date, NPM is the most common partner in ALCL and echinoderm microtubule-associated protein-like-4 (EML4) is the main partner in NSCLC. In addition to the chromosomal rearrangements that result in ALK fusion genes, amplification of ALK gene and activating point mutations in the full length ALK gene have recently been reported in neuroblastoma,[11-13] inflammatory breast cancer,[14] and ovarian cancer.[15]

Multiple pharmaceutical companies have described ALK inhibitors (ALKi) at various stages of development. [16-24] Structures of ALKi in clinical development are depicted in Figure 1. Compound **1** (PF-02441066, crizotinib)[25-28] was approved in 2011 by the FDA to treat ALK-positive NSCLC patients. Other ALK inhibitors, including **3** (CH5424802, Roche/Chugai),[29-30] **5** (ASP3026, Astellas),[31] **2** (X-396, X-Covery),[32] AP26113 (Ariad Pharmaceuticals. Structure undisclosed; series exemplified as compound **6**),[33-34] Tesaro (structure undisclosed) and **15b** (LDK378, Novartis),[35a] are currently in Phase 1/2 clinical trials.

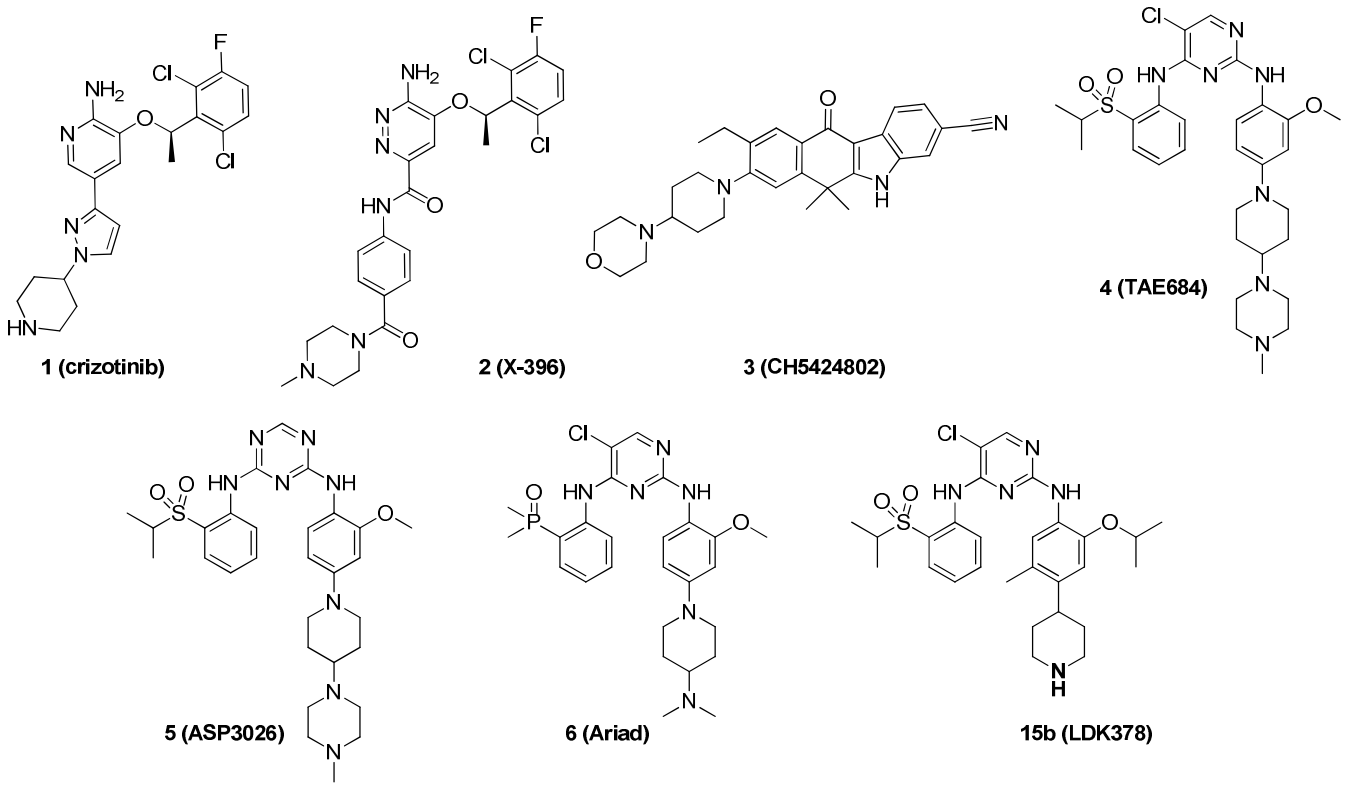

Figure 1. Structures of selected ALK inhibitors.

In this report, we describe the work we performed around the previously disclosed ALKi **4** (TAE684)[35b]. This research allowed us to find novel and selective ALK inhibitors with potent *in vivo* efficacy in ALCL and NSCLC rat xenograft models as well as improved development characteristics, leading to the discovery of compound **15b**.

Compound **4** is a potent ALK inhibitor; however, it was found to form an extensive number of reactive adducts upon metabolic oxidation, which creates the potential for significant toxicological liabilities. Semi-quantitative LC-MS analysis indicated that approximately 20% of **4** is converted into reactive species when incubated in liver microsomes (Table 2), and these reactive species can be trapped using glutathione (GSH).[36] Although no correlation was found between hepatotoxic drugs and the formation of GSH adducts,[37] it has been postulated that reactive metabolites may have a role in idiosyncratic[38] and/or other toxicities.[39]

A systematic evaluation of various compounds from the historical SAR dataset revealed that the reactive metabolite formation was primarily correlated with the presence of a solubilizing group connected by a nitrogen atom onto the central aniline moiety (Figure 2). It is hypothesized that metabolic oxidation of the electron-rich aromatic ring undergoes the formation of a 1,4-diiminoquinone moiety (A), which is highly reactive and forms adducts in the presence GSH (B).

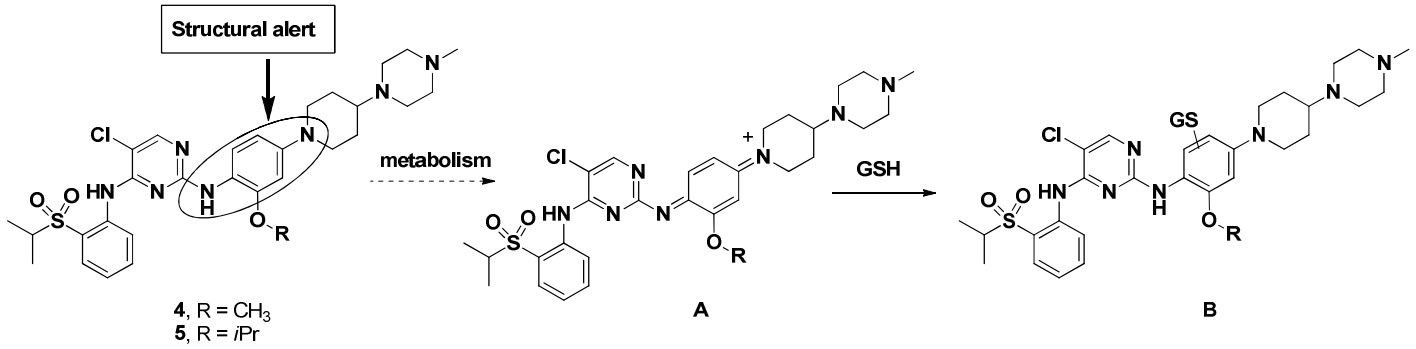

Figure 2. Hypothesized mechanism of reactive adduct formation from **4**.

Results and Discussion

Analogue Design and Chemistry. Based on modeling information,[35b] previous work in our laboratories have focused on increasing the kinase selectivity of **4** by modifying the methoxy moiety. This work resulted in finding that other alkoxy groups, such as an *iso*-propoxy moiety (**7**), was also well tolerated for ALK (Table 1) while having a positive effect on improved overall kinase selectivity

(supporting information, Figure S9) and reducing the potential metabolic liability associated with methoxy moieties.[40] However, it was also found the formation of reactive adducts observed with **7** and closely related analogues (unpublished results) was independent of the nature of alkoxy moiety present on the molecules (Table 2) confirming our hypothesis stated in Figure 2. With this information in hand, we took the decision to re-evaluate the SAR around this scaffold and focus our efforts towards the eradicating the reactive adducts that prevented **4** and some close analogues like **7** to enter into development. In order to reach this goal, we chose to retain the *iso*-propylsulfoneaniline as well as the *iso*-propoxy moieties, since these were shown to be important for potent and selective ALK inhibition. Variations on this theme were synthesized and profiled (*e.g.*, cyclobutylsulfoneaniline, *N,N*-dimethylsulfonamide) to determine the moiety with the best overall development profile. We also replaced the *iso*-propoxy with a cyclobutyloxy moiety, which is well-tolerated by ALK. For the compounds described in this report, we also kept the pyrimidine hinge-binding core constant, changing only the 5-chloro substituent to a 5-methyl in the case of compounds **18a-d**. As an additional point of comparison, **23**, which replaces the pyrimidine core with a pyridine, was synthesized. The focus of this report is on the SAR of the 4-position aniline 'tail' containing the solubilizing moiety. The SAR changes are highlighted in Figure 3. Additional, broader SAR explorations will be discussed in future publications.

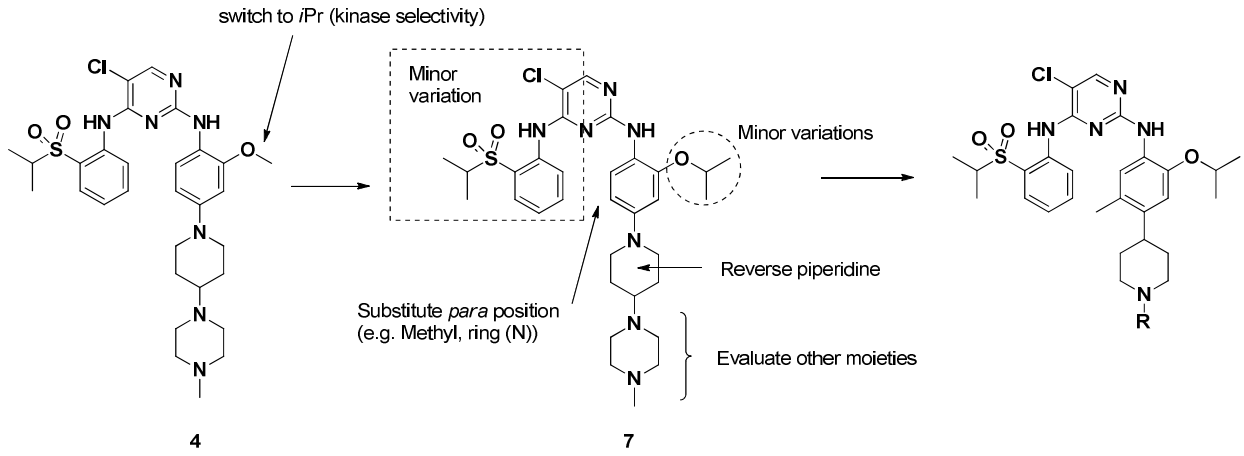

Figure 3. Structure-activity relationship overview.

With the aim of designing novel derivatives that would not form reactive adducts, we made the rational design decision to reverse the piperidine at the *para* position of the aniline moiety present in the series of compounds represented by **4** in order to remove the possibility of a 1,4-diiminoquinone formation. We also designed the inclusion of a methyl group *para* to the *iso*-propoxy moiety in order to further reduce metabolism on the interior phenyl ring, thereby further reducing the possibility of forming reactive metabolites.

The syntheses of the compounds **15a-e**, **16a,b**, **17a-i**, **18a-d**,**19**, **20** and **23** are shown in Schemes 1 and 2. The aniline moieties **8a-b** were synthesized in 2 steps from 2-fluoronitrobenzene according to a known procedure.[40] **8c** was synthesized in a very straightforward way from 2-nitrobenzenesulfonylchloride.[41] **8a-c** were then coupled to 2,3,5-trichloropyrimidine or 2,4-dichloro-5-methylpyrimidine to afford compounds **9a-d** in acceptable overall yield (40-61%). Anilines **13a-e** were synthesized in 4-8 synthetic steps from 2-chloro-4-fluorotoluene or 3-chlorofluorobenzene, while **13f** was synthesized from 2,4-dichloro-5-nitropyrimidine using an identical synthetic route. Nitration[39] of 2-chloro-4-fluorotoluene or 3-chlorofluorobenzene using KNO_3 in H_2SO_4 yielded the corresponding nitro derivatives **10a,b**. Condensation of **10a,b** with *iso*-propanol or cyclobutanol (60°C in the presence of K_2CO_3 in DMF/DMSO) afforded **10a-c** in excellent yield (>80%). Suzuki coupling of **11a-c** with 4-pyridineboronic acid afforded **12a-c** in >70% yield. *N*-methylation of **12b** followed by global reduction ($NaBH_4$ followed by PtO_2/H_2) generated **13d**. Alternatively, concomitant reduction of the pyridine and the nitro group present in **12a-c** using PtO_2/H_2 afforded the piperidine-aniline intermediates, which were subsequently protected, generating the Boc derivatives **13a-c** in good yields (>60%). Compound **13e** was synthesized by condensation of 2-methoxy-4-pyridylboronic acid onto **11b**, followed by demethylation of the methoxy group (refluxing conc. HCl in dioxane) and reduction of the pyridine ring (PtO_2/H_2). For the syntheses of **15a-e**, **16a,b**, **17a-i**, **18a-d** and **19-20**, **9a-d** were typically coupled to the aniline **13a-f** using a modified Buchwald coupling (Xantphos (10%), $Pd(OAc)_2$ (5%), Cs_2CO_3 (3 eq.), THF, MW, 150°C). Aside from **16a,b** and **19**, this was followed by Boc deprotection (TFA, CH_2Cl_2).

Finally, subsequent piperidine alkylation or acylation afforded **17a-i** and **18a-d** in good overall yields. Compounds **19** and **20** followed a similar synthetic route, except **9a** was coupled to 2-*iso*-propoxy-5-methyl-4-(2-oxopiperidin-4-yl)benzenaminium 2,2,2-trifluoroacetate for **19** and **13f** in the case of **20**. In order to synthesize compound **23**, we had to reverse the synthetic sequence. Amination of 4-bromo-2,5-dichloropyridine with **13a** (Xantphos, $Pd(OAc)_2$, Cs_2CO_3 , THF, MW, 150°C) afforded **22** in 41% yield**.** **22** was subsequently aminated with **8a (**$Pd_2(dba)_3$, dicyclohexyl(2,4,6- tri*iso*-propylphenyl)phosphine, NaO*t*Bu THF, MW, 150°C) to afford **23** in 11% yield.

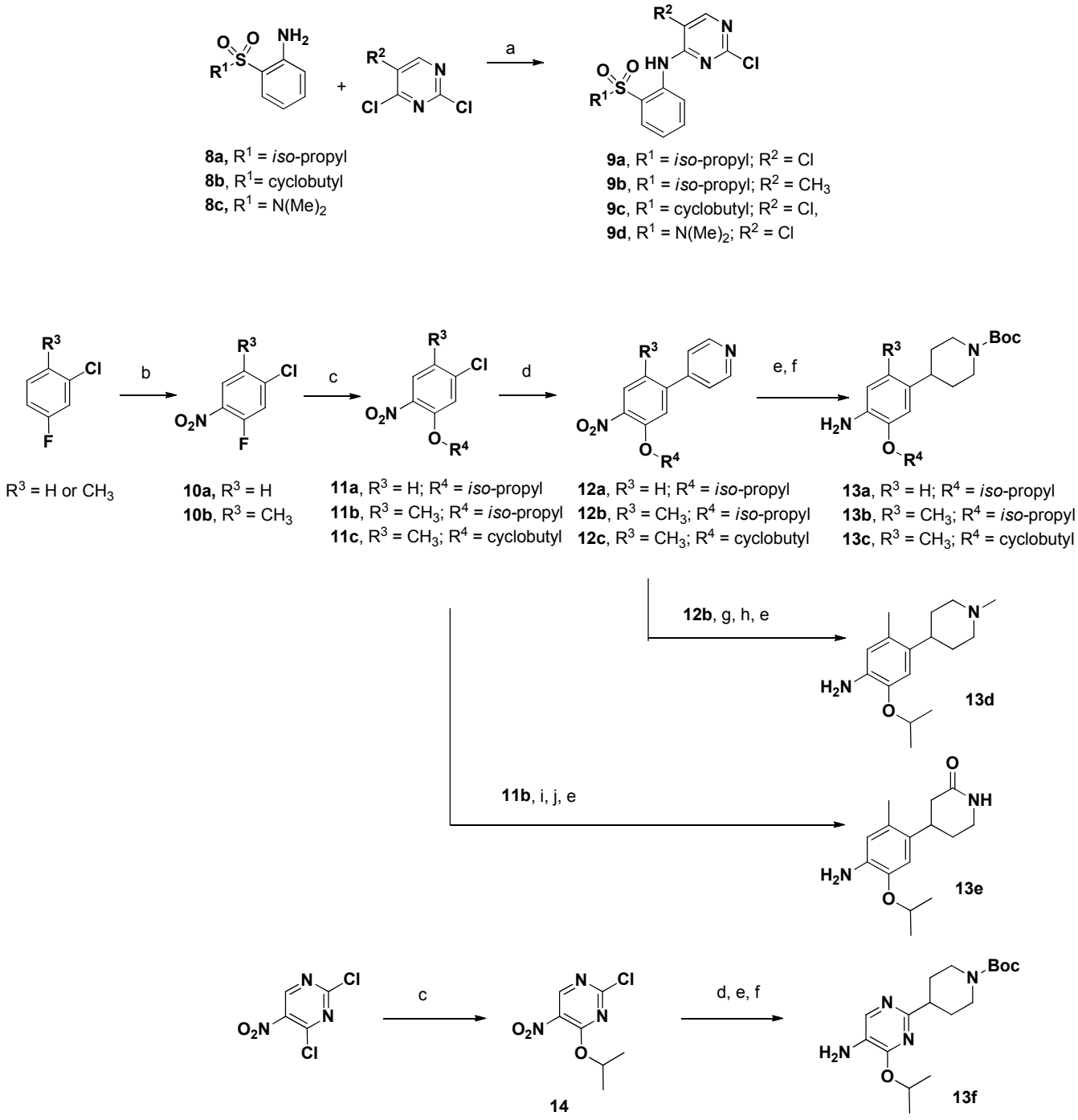

Scheme 1. Reagents and conditions: a. NaH, DMF/DMSO , 0℃ to 20℃ ; b. KNO_3, H_2SO_4, 0℃ to 20℃ c. Alcohol, Cs_2CO_3, 60℃. d. 4-Pyridineboronic acid, dioxane/H_2O or 1-BuOH ($Pd_2(dba)_3$, 2-dicyclohexylphosphine-2'-6'-dimethoxy biphenyl, MW, 150℃. e. AcOH/TFA; PtO_2, H_2. f. Anhydrous CH_2Cl_2, TEA, Boc_2O, 20℃. g. CH_3I, THF, 40°C, sealed tube. h. $NaBH_4$, CH_3OH, 0°C to 20°C. i. (2-methoxypyridin-4-yl)boronic acid, Pd_2dba_3, 2-dicyclohexylphosphine-2'-6'-dimethoxy biphenyl, K_3PO_4, 1-BuOH, 150°C. j. Concentrated HCl, dioxane, reflux.

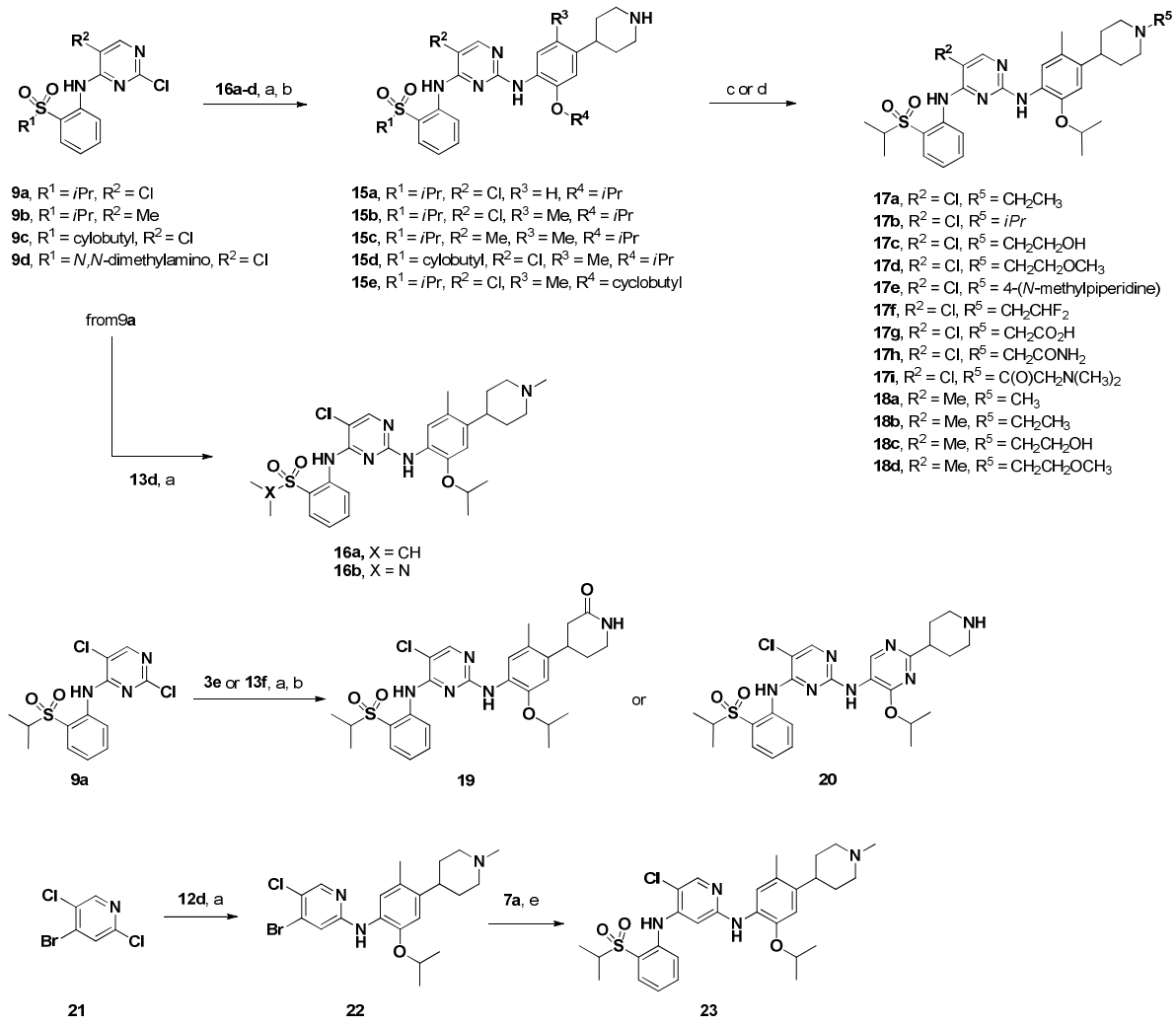

Scheme 2. Reagents and conditions: a. Xantphos, $Pd(OAc)_2$, Cs_2CO_3 , THF, MW, 150°C. b. TFA, CH_2Cl_2, 20°C. c. R-Br (or R-I), Et_3N, DMF, 20°C. d. $ClC(O)CH_2N(Me)_2 \cdot HCl$, pyridine, 20°C. e. $Pd_2(dba)_3$, dicyclohexyl(2,4,6-tri*iso*propylphenyl)phosphine, NaO*t*Bu THF, MW, 150°C.

In Vitro SAR.

Table 1 shows the *in vitro* cellular activity of compounds **15a-e**, **16a,b**, **17a-i**, **18a-d**,**19-20** and **23** against Ba/F3-NPM-ALK, Ba/F3-Tel-InsR and in Karpas299 cells. Since we had very potent starting points (compounds **4** and **7**) for this second-generation ALK inhibitor project, we decided to evaluate ALK inhibition directly in a cellular context by measuring the proliferation of Ba/F3 cells expressing the NPM-ALK or Tel-InsR fusion protein. Wild-type (WT) Ba/F3 cells were used as counterscreen in order to check for nonspecific cytotoxicity or interference with co-expressed luciferase which was used

to monitor cell proliferation. Anti-proliferative activity was monitored using the Karpas299 cell line which is a well-established line isolated from ALK-positive ALCL tumors possessing the NPM-ALK fusion. The data for the compounds described in this report is summarized in Table 1 below.

	Ba/F3-NPM-ALK	Ba/F3-Tel-InsR	Ba/F3-WT	Karpas299
1	150.8 ± 17.8	1643 ±272.0	3479±180.0	64.2±6.0
4	3.7 ± 0.5	43.7 ± 7.3	1336±279.1	2.4±0.5
7	24.8±7.9	414.0±81.0	3395±600	25.5±7.6
15a	10.6±1.7	281.8±28.2	3013±154.0	7.8±2.8
15b	26.0±0.3	319.5 ±23.5	2477±448.0	22.8±0.3
15c	40.6 ± 5.5	541.5±54.0	2884±194.0	13.1±1.3
15d	38.1±2.2	197.2±26.2	2460±260.0	13.5±2.4
15e	17.3±5.9	510.0±50.0	2517±406.0	13.1±9.0
16a	11.5 ± 0.2	464 ± 42.0	3997±24.6	11.2 ± 0.1
16b	25.0±5.3	339.0±33.0	1190±110.0	14.3±0.7
17a	32.1±3.8	344.5±40.0	4120±475.0	11.1±0.9
17b	29.9±4.4	240.1±53.6	3855±215.0	14.5±1.1
17c	8.1±2.3	326.5±58.5	4336±285.0	8.1±0.8
17d	43.5±6.0	349.0±38.5	4973±310.0	16.1±1.6
17e	258.4±49.7	1186±92.5	1420±107.5	100.3±19.3
17f	305.7±105.2	4874±290.0	>10000	293.5±81.0
17g	88.9±20.9	891.5±106.0	>10000	15.3±0.6
17h	16.5±3.2	361.1±42.3	7543±1050	7.9±0.3
17i	25.8±3.4	416.0±49.0	2737±113.0	21.7±5.9
18a	14.6±2.6	375.3±24.6	4077±173.3	15.6±1.8
18b	29.4±3.6	401.0±32.0	4005±480.0	10.5±0.6

18c	63.6±6.9	1643±126.0	>10000	23.8±2.0
18d	44.0±5.0	418.0±31.0	4407±290.0	22.4±1.6
19	48.3 ±7.8	784.0±112.0	> 10000	38.4±4.0
20	36.4±4.6	564.0±74.0	3800±200.0	33.3±4.3
23	4240±1360	1920±890.0	5412±330.0	5510±2190

Table 1. Activity profile of compounds **1**, **4**, **7**, **15a-e**, **16a,b**, **17a-i**, **18a-d**, **19-20** and **23**. All data given in nM and are an average of at least duplicate measurements.

Compound	GSH-trapping result
4	~20%
7	~19%
15b	<1%
15e	<1%
17a	<1%
17e	<1%
18a	<1%

Table 2. GSH-trapping results of derivatives **4**, **7**, **15b**, **15e**, **17a**, **17e** and **18a**.

Overall, most substitutions on the nitrogen of the piperidine were fairly well-tolerated (most cellular IC_{50}'s against ALK ranged from 10 to 50 nM). Among the compounds tested, derivatives such as **15a**, **16a** and **17c** approached the potency of compound **4** and were more potent than **7**. They were only approximately 2-3-fold less potent in the Ba/F3-NPM-ALK assay, and they possessed a better selectivity window versus the insulin receptor compared to **4** (InsR, 25- to 40-fold versus 11 and 15-fold for **4** and **7** respectively). Most compounds tested had an IC_{50} for NPM-ALK below 50 nM. However, it is interesting to note that addition of pKa-modulating moieties [such as a 2,2-trifluoroethyl group (**17f**)

or an acetic acid (**17g**)] decreased ALK inhibition activity. In contrast, addition of an acetamide (**17h**), a *N,N*-dimethylaminoacetate (**17i**), or conversion to a cyclic lactam (**19**) were well-tolerated for ALK inhibition and retained selectivity versus InsR. A similar trend was observed in the Karpas299 cell line. **23**, in which we replaced the pyrimidine core with a pyridine, resulted in a large loss of potency. This observation is consistent with the binding mode of these molecules in the ATP-binding site. The N^3 of the pyrimidine make a key contact at the hinge (Figure 4) and therefore, removing this key interaction considerably lowers affinity of compound **23**. We synthesized and profiled a number of minor variations of **15b** to identify the best development candidate. Substitutions in **15d**, **15e**, **16b**, and **20** were tolerated but did not show any significant development advantages over **15b**. A selected set of the compounds from Table 1 was tested in the GSH-trapping assay to evaluate their potential to form reactive adducts. The data are shown in Table 2. All the derivatives tested were found to have close to undetectable levels of GSH adducts (<1%) when submitted to the same assay conditions as **4** and **7** (supporting information, Figures S1-S4), experimentally confirming the validity of our rational designs.

Modeling and docking

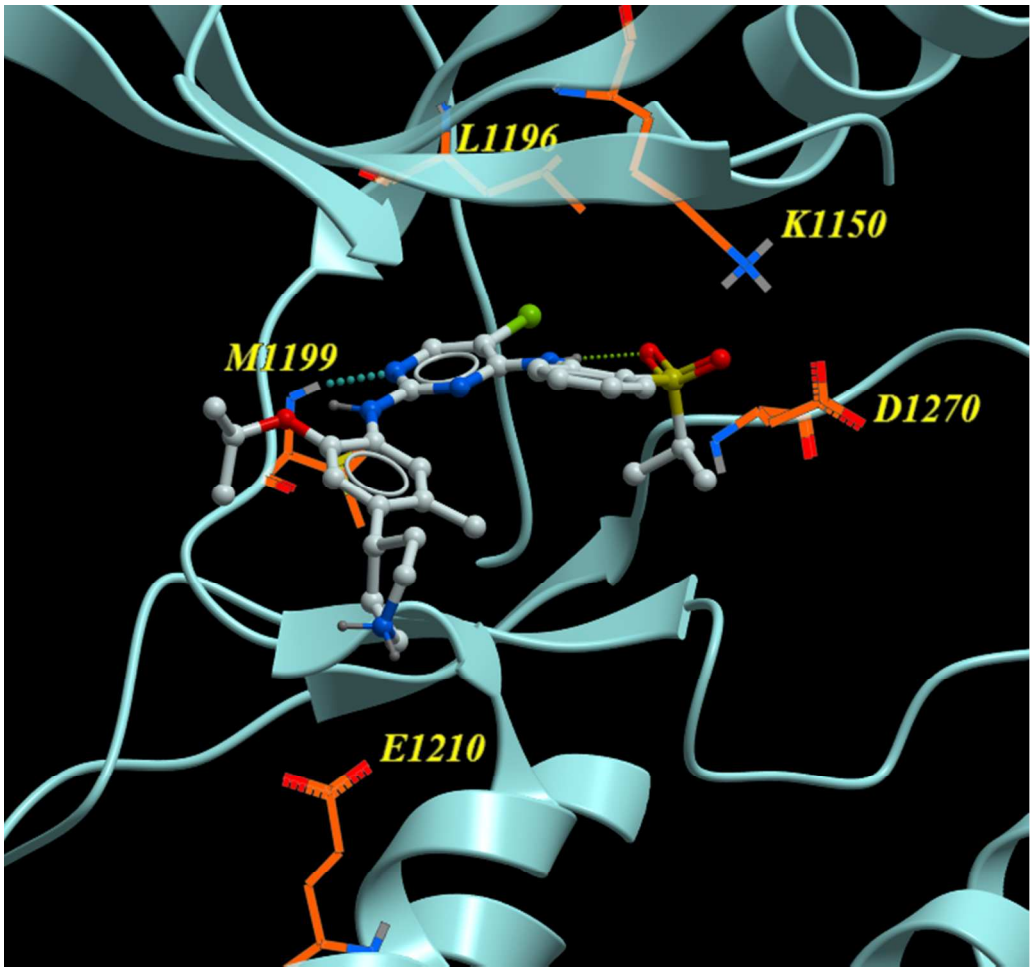

Figure 4. Docking of **15b** in the ALK kinase domain.

We performed molecular modeling of **15b** based upon the reported crystal structure of TAE684 with the kinase domain of ALK.[42] As expected, the ligand makes hydrogen bonds at the hinge area via the pyrimidine and amino nitrogen atoms onto the backbone nitrogen and oxygen of Met_{1199} respectively. Our model, shown in Figure 4, does not show the hydrogen bond between the carbonyl oxygen of Met_{1199} and the amino nitrogen of the inhibitor, even though they are within the range of a typical hydrogen bond, both distance- and angle-wise. The reason is that these two atoms occupy different planes, probably due to constraints of the crystal structure. We expect that they form a hydrogen bond in the context of a conformationally flexible protein in solution. The central pyrimidine ring of the inhibitor is sandwiched between Ala_{1148} and Leu_{1256} and its chlorine substituent is directed towards the back of the pocket making hydrophobic contact with gatekeeper Leu_{1196}. The piperidine ring extends to the solvent and is engaged in a salt bridge with Glu_{1210}. The sulfonyl makes an intramolecular H-bond

with the amine and is directed at Lys_{1150}. The *iso*propyl substituent bends down into the cavity formed by amino acids Arg_{1253}, Asn_{1254}, Cys_{1255}, Leu_{1256}, Gly_{1260}, and Asp_{1270}. The *iso*-propoxy group fits into a pocket formed by side chains of Arg_{1120} and Glu_{1132} and the Leu_{1198}-Ala_{1200}- Gly_{1201}-Gly_{1202} hinge segment.

While this model was not primarily used for compound optimization, it does correlate well with some of the SAR observations. For example, the lower potency of **17e** compared to **15b** may be explained by a greater number of rotatable bonds (entropic effect) present in **17e** as well as its greater mobility in the bound state. The latter follows from a difference in docking poses. In **15b**, the terminal piperidine fits closely to the protein surface and makes a salt bridge with E1210. In **17e**, by contrast, the corresponding central piperidine ring is pushed up into the solvent. This allows the formation of a salt bridge between its terminal piperidine and E1210 of the enzyme. The fact that **17e** has reduced surface contact with protein (see Figure S7 in supplementary information material) leads to its greater mobility. This can be demonstrated by conducting mixed Monte Carlo Multiple Minimum (MCMM)/LLMOD (Large Scale Low Mode) conformational search available in MacroModel 9.9 (Schrodinger, Inc, Portland, OR, 2012). The MCMM/LLMOD simulations revealed much greater mobility in the **17e** complex, especially in its terminal piperidine and the side chain of E1210 (see Figure S8 in supplementary information material). We hypothesize that this greater mobility of **17e** translates into its weaker binding potency.

ADME SAR. A selected set of these derivatives were evaluated for their ADME properties. Table 3 shows a summary of liver microsome intrinsic clearance, CYP3A4 inhibition, high throughput (HT) solubility as well as hERG inhibition (dofetilide binding assay) for **15a,b**, **15e**, **17a**, **16c**, **16i**, **17a** and **19**. The selected compounds have relatively good metabolic stability when tested in liver microsomes.[43] Moderate CYP3A4 (Midazolam substrate) inhibition was observed for these derivatives without a clear

SAR trend. A wide range of solubility values was observed, which was largely dependent on the pKa of the amine appended to the molecule. As expected, some hERG inhibition was also seen (again correlating well with the pKa of the amine moiety). hERG patch clamp experiments showed an IC_{50} of 46 and 20 μM respectively for **15b** and **18a**. Compound **15b** was further evaluated *in vivo* in both dog and monkey telemetry studies, and no evidence of QTc prolongation was observed (data not shown).

compound	CL_{int} m, r, h[1]	CYP3A4[2]	HTsol.[3]	hERG[4]
15a	15, 15, 15	1.4 ± 0.2	4	5.3
15b	15, 10, 19	1.5 ± 0.3	24	1.25[5]
15e	15, 15, 15	7.3± 0.8	<2	3.02
16a	15, `4, 17	2.1± 0.4	64	3.35
17c	15, 14, 15	2.5± 0.2	36	2.64
17i	45, 21, 46	0.6± 0.1	4	24.5
18a	15, 14, 8	9.8 ± 1.2	144	1.1[5]
20	21, 18, 16	9.3± 0.8	138	0.4

Table 3. ADME profile of selected derivatives. [1]Clearance (CL_{int}) is in μL/min/mg in liver microsomes. [2]Data in μM. Inhibition measured using midazolam as substrate. [3]Data in μM measured from DMSO solution in buffer adjusted to pH 6.8. [4]Data in μM in hERG dofetilide binding assay. [5]Follow-up hERG patch clamp data is shown in the body of paper.

Full *In Vitro* and *In Vivo* Profiling of 15b Additional profiling of compound **15b** for its kinase selectivity and pharmacokinetic profile was performed. Tables 4 and 5 display a selected enzymatic and cellular kinase profile of **15b** and Table 6 displays its PK profile in mouse, rat, dog and monkey. Compound **15b** displays a remarkable selectivity profile when tested against an enzyme panel of 46 kinases, showing biochemical inhibition below 100 nM for only three kinases: IGF-1R, InsR and

STK22D with IC_{50}'s of 8, 7 and 23 nM respectively. Compound **15b** is very potent against ALK at the enzymatic level (IC_{50} of 200 pM) thus its selectivity against these off-targets is 80-, 70- and 230-fold, respectively. When tested in a cellular proliferation panel of 39 kinases, **15b** proved to be very selective. Aside from ALK, no inhibition below 100 nM was observed for all kinases tested and the potent inhibitions observed for IGF-1R and FLT3 at the enzymatic level proved to be non-reproducible in a cellular context (IC_{50} of 410 and 3143 nM respectively). Likewise, cellular inhibition of FGFR2 and FGFR4 was found to be > 2 μM. We could not establish a cellular assay for STK22D but its inhibition was deemed to not be prohibitive for clinical development.

kinase	IC50 (μM)	Kinase	IC50 (μM)	kinase	IC50 (μM)
ABL	1.25	FGFR4	0.95	LYN	0.84
AKT	>10	FLT3	0.06	cMET	3.17
ALK	0.0002	GSK3β	>10	MKNK2	2.24
AURORA	0.66	GSK3β	>10	PAK2	>10
BTK	3.36	IGF-1R	0.008	PDGFRα	1.14
CDK2	3.97	InsR	0.007	RET	0.4
CDK4	4.72	JAK1	3.73	ROCK2	1.27
EGFR	0.9	JAK2	0.61	SYK	3.05
FGFR2	0.26	cKit	1.28	STK22D	0.023
FGFR3	0.43	LCK	0.56	ZAP70	9.7

Table 4. Enzymatic kinase profile of **15b.**

kinase	IC50 (nM)	Kinase	IC50 (nM)	kinase	IC50 (nM)
Tel-ALK	40.7±5.3	Tel-JAK2	2160±320	Tel-RET	2304±459

EML4-ALK	2.2±0.5	Tel-KDR	4210±170	Tel-Ros	141.8±22.7
Tel-FGFR3	>10000	Tel-ckit	2855±215	Tel-Src	1694±276
Tel-FGR	1947±433	Tel-Lck	672±264	Tel-TRKA	2727±222
Tel-FLT3	3143±933	Tel-LYN	2306±552	Tel-TRKB	1829±80
Tel-IGF-1R	410±10	Tel-Met	1339±74	Tel-WT	3250±710

Table 5. Cellular kinase profile of **15b** in Ba/F3 cells.

Compound **15b** was tested in mouse, rat, dog and monkey for its PK profile (Table 6). The compound exhibited low plasma clearance in animals (mouse, rat, dog and monkey) compared to liver blood flow. The volume of distribution at steady state (V_{ss}) was high and approximately 10-fold greater than total body water. Half-life ($T_{1/2}$) ranged from moderate to long (6.2 to 26 hrs). Following a single oral administration of **15b** as a solution or suspension, the oral bioavailability was good (≥55%) in mouse, rat, dog and monkey. Time of maximal concentration (T_{max}) occurred consistently late in animal species tested, indicating slow oral absorption. Overall, **15b** displays a consistent PK profile across all species tested. Although compound **15a**, which deletes the methyl *para* to the alkoxy group in **15b**, was fully tolerated by ALK, **15a** displayed significantly worse oral bioavailability in rat compared to **15b** (12%F vs. 66%F).

Species	Mouse		Rat		dog		Monkey	
Parameter	IV[1]	PO[1]	IV[1]	PO[1]	IV[2]	PO[3]	IV[2]	PO[4]
Dose (mg/kg)	5	20	3	10	5	20	5	60
AUC (hrs*nM)	5634	12296	2779	6092	18096	6790 4	11305	763 25
CL (mL/min/kg)	26.6	-	36.8	-	9.2	-	12.8	-

Vss (L/kg)	9.7	-	21.2	-	13.5	-	15	-
Cmax (nM)	1756	696	770	259	2329	1899	2526	1697
Tmax (h)	0.03	7.0	0.03	7.0	0.03	8.0		13
T1/2 (h)	6.2	-	9.1	-	21		26	
F(%)	-	55	-	66	-	119	-	56

Table 6. Mouse, rat, dog and monkey PK parameters of **15b**.[1] Formulated in a solution of 75% polyethylene300 and 25% dextrose (5%) in water.[2] Formulated in a solution of 30% propylene glycol and 5% Solutol® in phosphate-buffered saline [3] Formulated in a suspension of 0.5% (w/v) aqueous methylcellulose and 0.5% Tween 80.[4] Formulated in a suspension of 0.5% (w/v) aqueous methylcellulose.

Compound **15b** was tested for *in vivo* efficacy in 2-week Karpas299 (sc injection of Karpas299 cells possessing the NPM-ALK fusion) and H2228 (sc injection of H2228 cells possessing the EML4-ALK fusion) rat xenograft models. Doses were chosen to be 6.25, 12.5, 25 and 50 mg/kg daily dosing for the Karpas299 study and 5, 10, and 25 mg/kg daily dosing for the H2228 study. The efficacy of **15b** in these two models is summarized in Figures 6a and 6b. In the Karpas299 study, **15b** induced a dose-dependent growth inhibition (Tumor growth inhibition factor [T/C] = 74% at 6.25 mg/kg; T/C = 30% at 12.5 mg/kg) and tumor regression (T/C = -33% at 25 mg/kg and T/C = -66% at 50 mg/kg). In the H2228 study, **15b** induced a dose-dependent growth inhibition (T/C = 67% at 5 mg/kg; T/C = 2% at 10 mg/kg) and complete tumor regression at 25mg/kg (T/C = -100% at 25 mg/kg). In both models, **15b** was well tolerated and no body-weight loss was observed at all doses tested (Figures S5 and S6, supporting information). These

results are consistent with our previous observations (Karpas299 is a much more aggressive *in vivo* model than H2228) as well with the relative potency of **15b** against the NPM-ALK and EML4-ALK fusions (26.0 and 2.2 nM respectively)

A single-dose PK/PD experiment was performed in the rat Karpas299 model at 50 mg/kg, and the biomarker pSTAT3 response correlated well with the tumor regression observed in the xenograft study. Figure 7 shows the plot of plasma and tumor drug concentrations (left-hand side of the graph) versus pSTAT3 inhibition (right-hand side of the graph). Upon single-dose oral administration at 50 mg/kg, sustained pSTAT3 inhibition (about 80%) was observed through 72 hours, which paralleled the sustained tumor concentrations of **15b**.

In contrast to the first-generation ALK inhibitor **4**, compound **15b** showed no impact on insulin levels or plasma glucose utilization (tested via an oral glucose tolerance test) in the mouse upon chronic dosing up to 100 mg/kg (data not shown). This lack of *in vivo* effect on insulin receptor was confirmed using a homeostasis model assessment of insulin resistance (HOMA-IR; OGTT/ITT ratio) in the same animals (Figure 8). This *in vivo* selectivity is not fully understood at this time (the *in vitro* selectivity versus the InsR is comparable between **4** and **15b**) but indicates an additional advantage of **15b** over **4**.

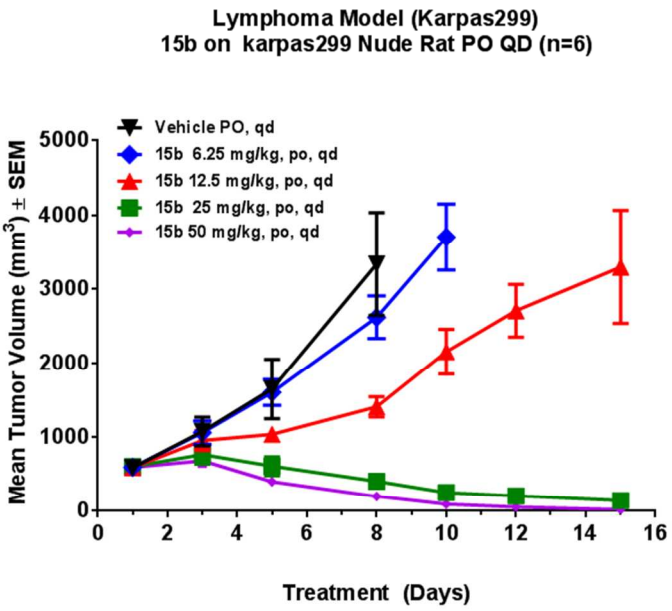

Figure 6a

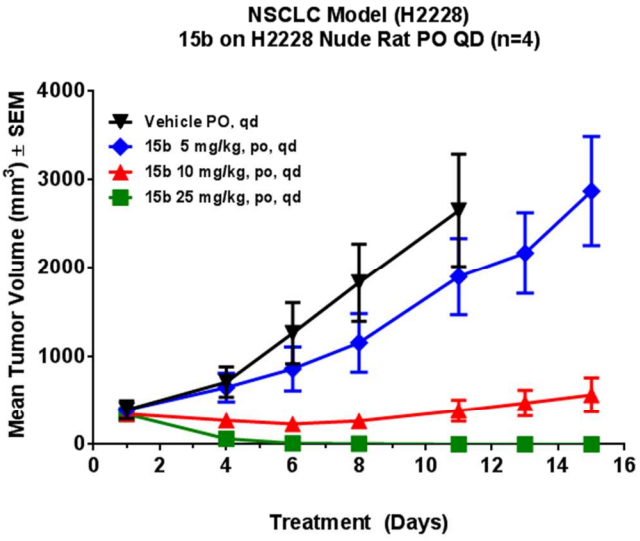

Figure 6b

Figure 6. a. Efficacy of **15b** in a 14-day rat xenograft Karpas299 model. b. Efficacy of **15b** in a 14-day rat xenograft H2228 model.

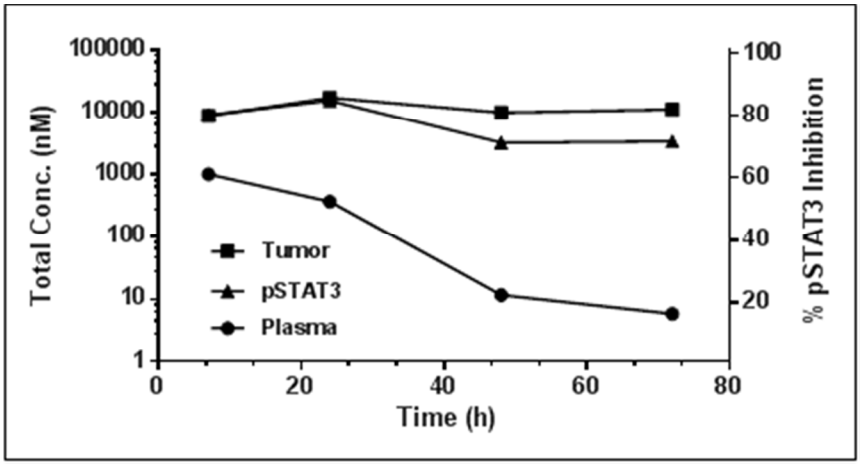

Figure 7. Single-dose PK/PD relationship of **15b** (50 mg/kg) in the rat Karpas299 model.

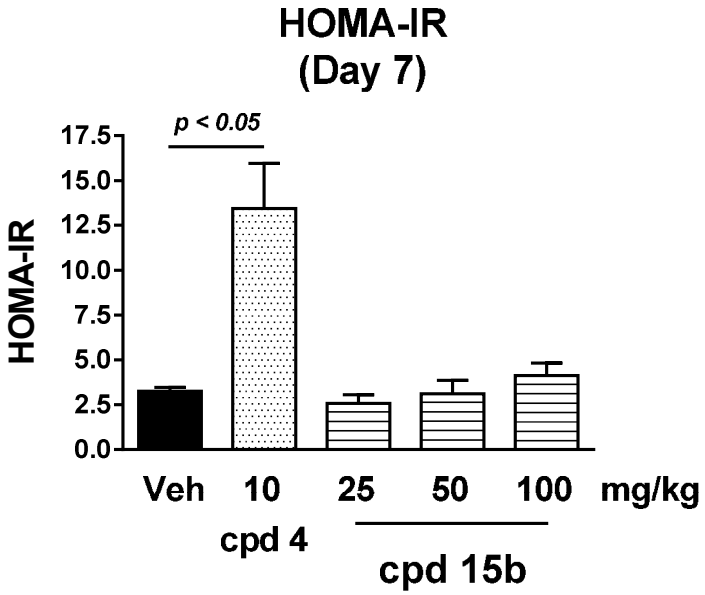

Figure 8. HOMA-IR result of **15b** and **4** after 7 days of dosing in mice.

Conclusions

In conclusion, we have described the synthesis of novel, selective and potent ALK inhibitors. Medicinal chemistry intuition and rational design were used to specifically and successfully address the extensive reactive adduct formation liability present in the first-generation clinical candidate **4.** Compound **15b** proved to have an acceptable overall profile (selectivity, ADME), a

consistent PK profile across species (mouse, rat, dog and monkey) and displayed strong *in vivo* efficacy in ALCL and NSCLC cancer xenograft models at well-tolerated doses. Compound **15b** also showed an improved profile in terms of *in vivo* glucose homeostasis over **4** when examined in mouse OGTT experiments. For these reasons, compound **15b** was chosen to move into development and is currently being evaluated in ALK-positive patients[44] where it has displayed substantial preliminary antitumor clinical activity.[45]

Experimental section

Unless otherwise noted, materials were obtained from commercial suppliers and were used without further purification. Removal of solvent under reduced pressure or concentration refers to distillation using Bu□chi rotary evaporator attached to a vacuum pump (3 mmHg). Products obtained as solids or high boiling oils were dried under vacuum (1 mmHg).

Purification of compounds by preparative RP-HPLC was achieved using a Waters autopurification system consisting of a 2767 autosampler/fraction collector, a 2525 binary gradient module, a 2487 UV detector, and a ZQ mass spectrometer. Compounds were purified using flow rate of 30 mL/min with a 50 mm × 20 mm i.d. Ultra 120 5 μm C18Q column (Peeke Scientific, Novato, CA). A 7.5 min linear gradient from 10% solvent A (acetonitrile with 0.035% trifluoroacetic acid) in solvent B (water with 0.05% trifluoroacetic acid) to 30-90% A was used, followed by a 2.5 min hold at 90% A. Silica gel chromatography was performed either by CombiFlash (separation system Sg. 100c, ISCO) or using silica gel (Merck Kieselgel 60, 230–400 mesh). Elemental analyses were carried out by Midwest Microlabs LLC, Indianapolis, IN. ^{1}H NMR spectra were recorded on Bruker XWIN-NMR (400 MHz) spectrometer. Proton

resonances are reported in parts per million (ppm) downfield from tetramethylsilane (TMS). ^{1}H NMR data are reported as multiplicity (s, singlet; d, doublet; t, triplet; q, quartet; quint, quintuplet; sept septuplet; dd, doublet of doublets; dt, doublet of triplets; bs, broad singlet). For spectra obtained in CDCl3, DMSO-*d*6, CD3OD, the residual protons (7.27, 2.50, and 3.31 ppm, respectively) were used as the internal reference.

Purity of Compounds

All compounds were analyzed with a Waters ZQ 2000 LC/MS system, which used an Agilent binary pump and photodiode array detector (PDA) along with a Sedere 75 evaporative light scattering detector (ELSD). Samples were injected from 96-well or 384-well plates with a Leap Technologies HTS Pal autosampler. The mobile phases used were (A) H2O + 0.05% TFA and (B) acetonitrile + 0.035% TFA. A gradient HPLC method with flow of 1.0 mL/min started at 5% B, with a hold of 0.1 min before a linear increase to 95% B at 2.70 min. At 2.71 min the B mobile phase was increased to 100% and held until 2.98 min. Total run time was 3.0 min. The column used was a Waters Atlantis dC18 2.1 mm × 30 mm, 3 μm. The mass spectrometer was operated in positive mode, with a spray voltage of 3.2 kV and cone voltage of 30 V. The source and desolvation temperatures were 130 and 400 °C, respectively, with 600 L/h of nitrogen desolvation flow. The progress of reactions and the purity of products were measured using 254 and 220 nm wavelengths and electrospray ionization (ESI) positive mode. Mass spectra were obtained in ESI positive mode. All the reported compounds were found to be >95% when analyzed at the 254 nm wavelength.

Synthesis of 2-chloro-N-(2-(*iso*-propylsulfonyl)phenyl)-5-methylpyrimidin-4-amine **9b**

To a suspension of 730 mg of NaH in a mixture of DMF/DMSO (25/2.5 ml) was added drop-wise at 0°C 2.53 g (12.69 mmol) of 2-(*iso*-propylsulfonyl)benzenamine **8a** in DMF/DMSO (10 ml, ratio 9/1). The solution was stirred for 30 minutes at 0°C and then 4.11 g (25.3 mmol, 2 eq.) of 2,4-dichloro-5-methylpyrimidine diluted in 10 ml of DMF/DMSO (ratio: 9/1) was added slowly. The solution was warmed to room temperature and stirred overnight. After aqueous work-up, the crude product was directly crystallized from cold CH_3CN in several batches to afford 2.53 g (7.75 mmol, 61%) of 2-chloro-N-(2-(*iso*-propylsulfonyl)phenyl)-5-methylpyrimidin-4-amine **9b** as pale creamy colored crystals: ESMS m/z 326.1 ($M + H^+$). ^1H NMR (400 MHz, DMSO-*d*6): δ 9.29 (s, 1H), 8.41 (dd, J = 0.9, 8.3 Hz, 1H), 8.23 (d, J = 0.8 Hz, 1H), 7.93 – 7.78 (m, 2H), 7.48 – 7.37 (m, 1H), 3.58 – 3.43 (m, 1H), 2.18 (s, 3H), 1.16 (d, J = 6.8 Hz, 6H).

Synthesis of 2,5-dichloro-N-(2-(*iso*-propylsulfonyl)phenyl)pyrimidin-4-amine **9a**

Using the same procedure described for the synthesis of 2-chloro-N-(2-(*iso*-propylsulfonyl)phenyl)-5-methylpyrimidin-4-amine **9b**, 2,5-dichloro-N-(2-(*iso*-propylsulfonyl)phenyl)pyrimidin-4-amine **9a** was isolated in 60% yield as a creamy colored solid from **8a** and 2,4,5-trichloropyrimidine: ESMS m/z 346.0 ($M + H^+$). ^1H NMR (400 MHz, DMSO-*d*6): δ 9.81 (s, 1H), 8.57 (s, 1H), 8.32 (d, J = 8.3 Hz, 1H), 7.96 – 7.82 (m, 2H), 7.56 – 7.42 (m, 1H), 3.61 – 3.46 (m, 1H), 1.16 (d, J = 6.8 Hz, 6H).

Synthesis of 2-chloro-4-fluoro-5-nitrotoluene **10b**.

To a solution of 100 g (0.7 mol) of 2-chloro-4-fluorotoluene in 250 ml of concentrated H_2SO_4 was added portion-wise 85 g (0.875 mol) of KNO_3 at 0°C (addition of the total amount of KNO_3

was complete in about 1 hour). The reddish mixture was slowly warmed to room temperature, stirred overnight, then poured over crushed ice and extracted with EtOAc. The organic layers were combined, dried over $MgSO_4$ and concentrated. The crude oil was purified over a large silica plug (eluent: 97/3 hexanes/EtOAc) to afford 94.7 g (0.5 mol, yield: 71%) of 2-chloro-4-fluoro-5-nitrotoluene **10b** as a pale yellow oil that solidifies upon standing. ^{1}H NMR ($CDCl_3$, 400 Mz): δ 7.97 (d, J = 8.0 Hz, 1H), 7.32 (d, J = 10.4 Hz, 1H), 2.43 (s, 3H).

Synthesis of 2-chloro-4-*iso*-propoxy-5-nitrotoluene **11b**

To a solution of 25 g (0.131 mol) of 2-chloro-4-fluoro-5-nitrotoluene **10b** in 250 ml of 2-propanol was added 208 g (0.659 mol, 5 eq.) of Cs_2CO_3. The mixture was stirred at 60^{o}C overnight and after cooling to room temperature, most of the 2-propanol was evaporated under reduced pressure. Water was added and the solution was extracted with EtOAc. The organic layers were combined, dried over $MgSO_4$, concentrated and the crude product filtered through a silica plug (eluent: 95/5 hexanes/EtOAc) to afford 28.7 g (0.125 mol, 95%) of 2-chloro-4-*iso*-propoxy-5-nitrotoluene **11b** as a pale yellow fluffy solid. ^{1}H NMR (400 MHz, DMSO-*d*6): δ 7.90 (d, J = 0.6 Hz, 1H), 7.52 (s, 1H), 4.92 – 4.76 (m, 1H), 2.30 (s, 3H), 1.27 (d, J = 6.0 Hz, 6H).

Synthesis of 4-(5-*iso*-propoxy-2-methyl-4-nitro-phenyl)-pyridine **12b**

4-Pyridineboronic acid (147 mg, 1.20 mmol, 1.1 eq.) was dissolved in a 2:1 v/v mixture of dioxane and H_2O (15 mL) and N_2 was bubbled through for 5 minutes. Pd_2dba_3 (100 mg, 0.109 mmol, 0.1 eq.), 2-dicyclohexylphosphine-2'-6'-dimethoxy biphenyl (112 mg, 0.272 mmol, 0.25 eq.), 1-chloro-5-*iso*-propoxy-2-methyl-4-nitro-benzene (**11b**, 250 mg, 1.09 mmol, 1.0 eq.) and K_3PO_4 (462 mg, 2.18 mmol, 2.0 eq.) were added under a N_2 blanket. The reaction vessel was

sealed and heated with microwave irradiation to 150°C for 20 min. After cooling to room temperature, the reaction was diluted with ethyl acetate and washed twice with 1 N aqueous NaOH. The organic layer was then dried over Na_2SO_4 and filtered. After concentration, the crude product was purified by silica gel chromatography (gradient from hexanes to 30% ethyl acetate in hexanes) to give 217 mg (0.798 mmol, 73%) of 4-(5-*iso*-propoxy-2-methyl-4-nitro-phenyl)-pyridine (**12b**) as a brown solid. ESMS m/z 273.1 ($M + H^+$).

Synthesis of 2-*iso*-propoxy-5-methyl-4-(1-methyl-piperidin-4-yl)-phenylamine (**13d**)

4-(5-*iso*-propoxy-2-methyl-4-nitro-phenyl)-pyridine (**12b**, 217 mg, 0.798 mmol) was dissolved in anhydrous THF (9 mL). Iodomethane (0.10 mL, 1.61 mmol, 2 eq.) was added and the reaction was stirred at 40°C in a sealed tube for 2 days. The volatiles were removed under vacuum generating 4-(5-*iso*-propoxy-2-methyl-4-nitro-phenyl)-1-methyl-pyridinium iodide as a brown solid directly used in the next step: ESMS m/z 287.1 (M+).

4-(5-*iso*-propoxy-2-methyl-4-nitro-phenyl)-1-methyl-pyridinium iodide (0.80 mmol) was dissolved in CH_3OH (20 mL) and cooled to 0°C. $NaBH_4$ (302 mg, 8.0 mmol, 10 eq.) was slowly added. After this addition was complete, the cooling bath was removed and the reaction was stirred at room temperature for 2.5 h. The reaction was quenched by the slow addition of 1N aqueous HCl (14 mL). The CH_3OH was partially removed by vacuum and the resulting residue was partitioned between EtOAc and 1 N aqueous NaOH. Additional 50% aqueous NaOH was added until the aqueous layer pH>12. The EtOAc layer was washed twice with 1 N aqueous NaOH, the organic layer was then dried over Na_2SO_4, filtered, and concentrated under vacuum. After concentration, the crude product (175 mg) was dissolved in acetic acid (10 mL). TFA (0.15 mL, 3 eq.) and PtO_2 (53 mg, 30% w/w) were added and the reaction was placed under 50

psi H_2 gas in a Parr Shaker for 14 h. The reaction mixture was filtered and the filtrate concentrated under vacuum. The resulting residue was partitioned between EtOAc and 1 N aqueous NaOH. Additional 50% aqueous NaOH was added until the aqueous layer pH>12. The EtOAc layer was washed with 1 N aqueous NaOH (2x), and then the organic layer was dried over Na_2SO_4, filtered, and concentrated under vacuum to give 2-*iso*-propoxy-5-methyl-4-(1-methyl-piperidin-4-yl)-phenylamine **13b** (161 mg, 77%): ESMS m/z 263.2 ($M + H^+$).

Synthesis of 4-(4-amino-5-*iso*-propoxy-2-methylphenyl)piperidin-2-one **13e**

1-chloro-5-*iso*-propoxy-2-methyl-4-nitrobenzene **11b** (275 mg, 1.20 mmol, 1.0 eq.) was dissolved in 1-butanol (6 mL) and N_2 is bubbled through for 5 minutes. Pd_2dba_3 (55 mg, 0.06 mmol, 0.05 eq.), 2-dicyclohexylphosphine-2'-6'-dimethoxy biphenyl (50 mg, 0.12 mmol, 0.1 eq.), (2-methoxypyridin-4-yl)boronic acid (239 mg, 1.56 mmol, 1.3 eq.) and K_3PO_4 (497 mg, 2.4 mmol, 2.0 eq.) were added under a N_2 blanket. The reaction vessel was sealed and heated at 150°C overnight. After cooling to room temperature, the solvent was removed under reduced pressure and the residue was purified by silica gel chromatography (gradient from 0% to 20% ethyl acetate in hexanes) to give 130 mg of 4-(5-*iso*-propoxy-2-methyl-4-nitrophenyl)-2-methoxypyridine as yellow oil. ESMS m/z 303.1 ($M + H^+$). ^1H NMR (CD_3OD, 400 Mz): δ 8.21 (d, J = 5.6 Hz, 1H), 7.70 (s, 1H), 7.08 (s, 1H), 6.96 (dd, J = 5.6, 1.6 Hz, 1H), 6.79 (s, 1H), 4.75 (m, 1H), 3.97 (s, 3H), 2.22 (s, 3H), 1.34 (d, J = 6.0 Hz, 6H).

Synthesis of 4-(5-*iso*-propoxy-2-methyl-4-nitrophenyl)-2-methoxypyridine (130 mg, 0.43 mmol) was dissolved in 1,4-dioxane (8.0 mL) and concentrated HCl (1.0 mL) was added. The resulting mixture was refluxed overnight. After cooling to room temperature, the solvent was removed under reduced pressure and the crude product, 4-(5-*iso*-propoxy-2-methyl-4-nitrophenyl)pyridin-2-ol, was used directly for the next step without further purification. ESMS

m/z 289.1 ($M + H^+$). ^1H NMR (CD_3OD, 400 Mz): δ 8.00 (d, J = 6.4 Hz, 1H), 7.65 (s, 1H), 7.12 (s, 1H), 7.05 (dd, J = 6.4, 1.6 Hz, 1H), 6.92 (d, J = 1.6 Hz, 1H), 4.70 (m, 1H), 2.19 (s, 3H), 1.26 (d, J = 6.0 Hz, 6H).

To the above product, 4-(5-*iso*-propoxy-2-methyl-4-nitrophenyl)pyridin-2-ol, in TFA (8.0 mL) was added PtO_2 (9.8 mg). The mixture was purged with H_2 and stirred at room temperature overnight under 1 atm. H_2 (g). After filtration through celite, the filtrate was concentrated to yield the crude product, 4-(4-amino-5-*iso*-propoxy-2-methylphenyl)piperidine-2-one **13e**, which was used directly for the next step without further purification. ESMS m/z 263.1 ($M + H^+$).

Synthesis of *tert*-butyl 4-(5-amino-4-*iso*-propoxypyrimidin-2-yl)piperidine-1-carboxylate **13f**

A degazed mixture of 109 mg (0.5 mmol) of 2-chloro-4-*iso*-propoxypyrimidin-5-amine, 230 mg (0.75 mmol) of *tert*-butyl 4-(4,4,5,5-tetramethyl-1,3,2-dioxaborolan-2-yl)-5,6-dihydropyridine-1(2H)-carboxylate, $Pd(OAc)_2$ (10 mg, 0.044 mmol), Xantphos (20 mg, 0.034 mmol), K_3PO_4 (350 mg, 1.5 mmol) in 1.5 mL of THF was heated to 85^{o}C for 24 hrs. After cooling at RT, the mixture was filtered, concentrated, dissolved in 5 mL of dry MeOH and 5 mg of Pd/C was added. The resulting mixture was flushed with N_2 and placed under H_2 atmosphere (balloon) ON. After filtration and concentration, the residue was purified over SiO_2 column to afford 20 mg (0.059 mmol, yield: 12%) of *tert*-butyl 4-(5-amino-4-*iso*-propoxypyrimidin-2-yl)piperidine-1-carboxylate **13f** as an oil. ESMS m/z 337.2 ($M + H^+$).

Synthesis of 4-(4-Amino-5-*iso*-propoxy-2-methyl-phenyl)-piperidine-1-carboxylic acid *tert*-butyl ester **13b**

Synthesis of 4-(5-*iso*-propoxy-2-methyl-4-nitro-phenyl)-pyridine **12b** (438 mg, 1.61 mmol) dissolved in acetic acid (30 mL) was treated with TFA (0.24 mL, 3.22 mmol) and PtO_2 (176 mg, 40% w/w). The reaction mixture was vigorously stirred under 1 atm. H_2 for 36 hours. The reaction mixture was filtered and the filtrate was concentrated under vacuum. The resulting residue was diluted with ethyl acetate and washed twice with 1 N aqueous NaOH, the organic layer was then dried over Na_2SO_4 and filtered. After concentration, the crude product (391 mg) was dissolved in anhydrous CH_2Cl_2 (30 mL). TEA was added (0.44 mL, 3.15, 2 eq.) followed by Boc_2O (344 mg, 1.6 eq.). The reaction was stirred at room temperature for 30 min. and then concentrated under vacuum. The resulting residue was purified by silica gel chromatography (gradient from hexanes to 30% ethyl acetate in hexanes) to give 4-(4-amino-5-*iso*-propoxy-2-methyl-phenyl)-piperidine-1-carboxylic acid *tert*-butyl ester **13b** (340 mg, 0.976 mmol, yield: 60% over 2 steps) as a sticky foam: ESMS m/z 293.1 (M-tBu+H^+). ^{1}H NMR (400 MHz, CD_3OD) δ 7.61 (s, 1H), 6.76 (s, 1H), 4.64 – 4.45 (m, 1H), 4.22 (d, J = 13.2, 2H), 2.90 (m, 3H), 2.28 (s, 3H), 1.73 (d, J = 12.2, 2H), 1.54 (d, J = 11.4, 2H), 1.52 (s, 9H),1.31 (d, J = 6.0, 6H).

Synthesis of 4-(4-Amino-5-*iso*-propoxy-2-methyl-phenyl)-piperidine-1-carboxylic acid *tert*-butyl ester **13a**

13a was synthesized according to the same procedure described for **13b** from 660 mg (3.40 mmol) of 2-*iso*-propoxy-4-(pyridin-4-yl)aniline **12a** in 58% overall yield (660 mg isolated; 1.97 mmol). ESMS m/z 335.2 (M + H^+).

Synthesis of *tert*-butyl 4-(4-amino-5-cyclobutoxy-2-methylphenyl)piperidine-1-carboxylate **13c**

13c was synthesized according to the same procedure described for **13b** from 270 mg (0.95 mmol) of 2-cyclobutoxy-5-methyl-4-(pyridin-4-yl)aniline **12c** in 80% overall yield (300 mg isolated, 0.84 mmol). ESMS m/z 361.2 ($M + H^+$).

Final molecules

Synthesis of 5-Chloro-N2-(2-*iso*-propoxy-5-methyl-4-piperidin-4-yl-phenyl)-N4-[2-(propane-2-sulfonyl)-phenyl]-pyrimidine-2,4-diamine **15b**

4-(4-Amino-5-*iso*-propoxy-2-methyl-phenyl)-piperidine-1-carboxylic acid tert-butyl ester (170 mg, 0.488 mmol) **13b**, (2,5-Dichloro-pyrimidin-4-yl)-[2-(propane-2-sulfonyl)-phenyl]-amine (**9a**, 169 mg, 0.488 mmol, 1 eq.), xantphos (28 mg, 0.049 mmol, 0.1 eq.), $Pd(OAc)_2$ (5.5 mg, 0.024 mmol, 0.05 eq.), and Cs_2CO_3 (477 mg, 1.46 mmol, 3 eq.) were dissolved in anhydrous THF (6 mL). N_2 was bubbled through the reaction mixture for 5 minutes and then the reaction vessel was sealed and heated under microwave irradiation to 150°C for 20 min. The reaction was filtered and the filtrate concentrated under vacuum. After concentration, the crude product was purified by silica gel chromatography (gradient from hexanes to 30% ethyl acetate in hexanes) to give 4-(4-{5-chloro-4-[2-(propane-2-sulfonyl)-phenylamino]-pyrimidin-2-ylamino}-5-*iso*-propoxy-2-methyl-phenyl)-piperidine-1-carboxylic acid *tert*-butyl ester as a yellow film (105 mg) which was directly used in the next step: ESMS m/z 658.3 ($M + H^+$). This product (105 mg, 0.160 mmol) was dissolved in CH_2Cl_2 (3 mL) and treated with TFA (3 mL). After 45 min., the reaction was concentrated under vacuum. 1 N HCl in Et_2O (5 mL x 2) was added causing the product HCl salt to precipitate. The solvent was removed by decantation. The resulting 5-Chloro-N2-(2-*iso*-propoxy-5-methyl-4-piperidin-4-yl-phenyl)-N4-[2-(propane-2-sulfonyl)-phenyl]-pyrimidine-2,4-diamine (**15b**) was dried under high vacuum, generating an

off-white powder (101 mg, 35% yield): ^{1}H NMR (400 MHz, DMSO-*d*6 + trace D_2O) δ 8.32 (s, 1H), 8.27 (d, 1H), 7.88 (d, 1H), 7.67 (dd, 1H), 7.45 (dd, 1H), 7.42 (s, 1H), 6.79 (s, 1H), 4.56-4.48 (m, 1H), 3.49-3.32 (m, 3H), 3.10-2.91 (m, 3H), 2.09 (s, 3H), 1.89-1.77 (m, 4H), 1.22 (d, 6H), 1.13 (d, 6H); ESMS m/z558.1 ($M + H^+$). Anal. Calcd for $C_{28}H_{36}ClN_5O_3S$: C, 60.25; H, 6.50; Cl, 6.35; N, 12.55; O, 8.60; S, 5.75. Found: C, 60.29; H, 6.45; N, 12.55 (Analytical sample of free base).

Synthesis of 5-chloro-N2-(2-*iso*-propoxy-4-(piperidin-4-yl)phenyl)-N4-(2-(*iso*-propylsulfonyl)phenyl)pyrimidine-2,4-diamine (**15a**)

5-chloro-N2-(2-*iso*-propoxy-4-(piperidin-4-yl)phenyl)-N4-(2-(*iso*-propylsulfonyl)phenyl)pyrimidine-2,4-diamine (**15a**) was synthesized in 29% overall yield (89 mg, 0.164 mmol) according to the same procedure described for **15b** from 199 mg (0.576 mmol) of **9a** and 214 mg (0.63 mmol) of **13a**. ^{1}H NMR (400 MHz, DMSO-*d*6 + trace D_2O) δ 8.33-8.26 (m, 2H), 7.85 (d, 1H), 7.66 (dd, 1H), 7.52 (d, 1H), 7.44 (dd, 1H), 6.90 (s, 1H), 6.68 (d, 1H), 4.63-4.53 (m, 1H), 3.45-3.30 (m, 3H), 3.04-2.93 (m, 2H), 2.86-2.76 (m, 1H), 1.99-1.87 (m, 2H), 1.82-1.68 (m, 2H), 1.21 (d, 6H) 1.12 (d, 6H); ESMS m/z 544.2 ($M + H^+$). HRMS for $C_{27}H_{34}ClN_5O_3S$; calcd: 544.2144, found: 544.2142.

Synthesis of N2-(2-*iso*-propoxy-5-methyl-4-(piperidin-4-yl)phenyl)-N4-(2-(*iso*-propylsulfonyl)phenyl)-5-methylpyrimidine-2,4-diamine (**15c**)

N2-(2-*iso*-propoxy-5-methyl-4-(piperidin-4-yl)phenyl)-N4-(2-(*iso*-propylsulfonyl)phenyl)-5-methylpyrimidine-2,4-diamine (**15c**) was synthesized in 56% overall yield (127 mg, 0.237 mmol) according to the same procedure described for **15b** from 138 mg (0.424 mmol) of **9b** and

123 mg (0.353 mmol) of **13b**. ^{1}H NMR (400 MHz, DMSO-d6) δ 9.79 (bs, 0.5H), 9.15 (bs, 0.5H), 8.75 (bs, 1H), 8.56 (bs, 1H), 8.02-7.87 (m, 3H), 7.73 (dd, 1H), 7.55 (dd, 1H), 7.23 (s, 1H), 6.75 (s, 1H), 4.56-4.44 (m, 1H), 3.04-2.84 (m, 3H), 2.48-2.44 (m, 3H), 2.12 (s, 3H), 1.95 (s, 3H), 1.85-1.69 (m, 4H), 1.19 (d, 6H) 1.05 (d, 6H); ESMS m/z 538.3 (M + H^+). HRMS for $C_{29}H_{39}N_5O_3S$; calcd: 538.2847, found: 538.2853.

Synthesis of 5-chloro-N4-(2-(cyclobutylsulfonyl)phenyl)-N2-(2-*iso*-propoxy-5-methyl-4-(piperidin-4-yl)phenyl)pyrimidine-2,4-diamine (**15d**)

5-chloro-N4-(2-(cyclobutylsulfonyl)phenyl)-N2-(2-*iso*-propoxy-5-methyl-4-(piperidin-4-yl)phenyl)pyrimidine-2,4-diamine (**15d**) was synthesized according to the same procedure described for **15b** from 36 mg (0.10 mmol) of 2,5-dichloro-N-(2-(cyclobutylsulfonyl)phenyl)pyrimidin-4-amine and 32.3 mg (0.10 mmol) of 2-*iso*-propoxy-5-methyl-4-(piperidin-4-yl)aniline in 35% overall yield (20 mg isolated, 0.035 mmol). ^{1}H NMR (400 MHz, CD_3OD) δ 8.43 (d, J = 8.0 Hz, 1H), 8.14 (s, 1H), 7.93 (dd, J = 1.5, 8.0 Hz, 1H), 7.73 (s, 1H), 7.68 – 7.61 (m, 1H), 7.38 – 7.30 (m, 1H), 6.85 (s, 1H), 4.65 – 4.53 (m, 1H), 4.07 – 3.96 (m, 1H), 3.20 – 3.12 (m, 2H), 2.91 – 2.81 (m, 1H), 2.81 – 2.71 (m, 2H), 2.52 – 2.39 (m, 2H), 2.19 –2.08 (m, 5H), 2.03 – 1.85 (m, 2H), 1.78 – 1.70 (m, 2H), 1.70 – 1.57 (m, 2H), 1.32 (d, J = 6.1 Hz, 6H). ESMS m/z (M+H+): 570.2. HRMS for $C_{29}H_{36}ClN_5O_3S$; calcd: 570.2300, found: 570.2304.

Synthesis of 5-chloro-N2-(2-cyclobutoxy-5-methyl-4-(piperidin-4-yl)phenyl)-N4-(2-(*iso*-propylsulfonyl)phenyl)pyrimidine-2,4-diamine (**15e**)

5-chloro-N2-(2-cyclobutoxy-5-methyl-4-(piperidin-4-yl)phenyl)-N4-(2-(*iso*-propylsulfonyl)phenyl)pyrimidine-2,4-diamine (**15e**) was synthesized according to the same procedure described for **15b** from 145 mg (0.42 mmol) of **9a** and 151 mg (0.42 mmol) of **13c** in 6% overall yield (15 mg, 0.059 mmol).^{1}H NMR (400 MHz, DMSO-*d*6) δ 9.74 (bs, 1H), 8.94-8.76 (m, 2H), 8.39-8.31 (m, 2H), 7.87 (d, 1H), 7.65 (dd, 1H), 7.47-7.38 (m, 2H), 6.63 (s, 1H), 4.69-4.59 (m, 1H), 3.09-2.92 (m, 3H), 2.44-2.32 (m, 3H), 2.11 (s, 3H), 2.16-1.98 (m, 3H), 1.96-1.69 (m, 6H), 1.66-155 (m, 1h), 1.15 (d, 6H); ESMS m/z 570.2 ($M + H^+$). HRMS for $C_{29}H_{36}ClN_5O_3S$; calcd: 570.2300, found: 570.2308.

Synthesis of 4-bromo-5-chloro-N-(2-*iso*-propoxy-5-methyl-4-(1-methylpiperidin-4-yl)phenyl)pyridin-2-amine (**22**) and 5-chloro-N2-(2-*iso*-propoxy-5-methyl-4-(piperidin-4-yl)phenyl)-N4-(2-(*iso*-propylsulfonyl)phenyl)pyridine-2,4-diamine (**23**)

A mixture of 52.4 mg (0.2 mmol) of 2-*iso*-propoxy-5-methyl-4-(1-methylpiperidin-4-yl)aniline **13d**, 59.1 mg (0.22 mmol) of 4-bromo-2,5-dichloropyridine, 8.8 mg (5 mol%) of $Pd(OAc)_2$, 28.8 mg (10 mol%) of Xantphos, and 130.4 mg of Cs_2CO_3 in 4.0 mL of anhydrous THF was heated at 150^{o}C for 40 min. under microwave irradiation. After cooling to room temperature and concentration, the residue was purified with silica gel column chromatography (eluent: 0-10% MeOH in CH_2Cl_2) to afford 38.0 mg (0.084 mmol, yield: 42%) of 4-bromo-5-chloro-N-(2-isopropoxy-5-methyl-4-(1-methylpiperidin-4-yl)phenyl)pyridin-2-amine **22** as a yellow oil. MS (ES+): 454.0 $(M+1)^+$.

A mixture of 38.0 mg (0.084 mmol of **22**, 20 mg (0.10 mmol) of 2-(*iso*-propylsulfonyl)aniline, 3.9 mg (5 mole%) of Pd2dba3, 4.0 mg (10 mol%) of dicyclohexyl(2,4,6-tri*iso*-

propylphenyl)phosphine, and 12 mg (0.168 mmol) of NaO*t*Bu in 1.0 mL of dry THF was heated to 150ºC under microwave irradiation. After concentration the residue was purified by preparative RP-HPLC to afford 5.5 mg (0.0096 mmol, yield: 11%) of 5-chloro-N2-(2-*iso*-propoxy-5-methyl-4-(piperidin-4-yl)phenyl)-N4-(2-(*iso*-propylsulfonyl)phenyl)pyridine-2,4-diamine **23** as an oil.^{1}H NMR (400 MHz, DMSO-*d*6) δ 9.21 (broad s, 1H), 8.47 (broad s, 1H), 7.94 (m, 2H), 7.67 (dd, J = 8.0, 1.2 Hz, 1H), 7.57 (m, 1H), 7.10 (m, 2H), 6.75 (s, 1H), 6.09 (s, 1H), 4.43 (m, 1H), 3.05 (m, 3H), 2.93 (m, 1H), 2.76 (m, 3H), 2.21 (s, 3H), 1.80 (m, 4H), 1.13 (d, J = 6.0 Hz, 6H), 1.04 (d, J = 6.8 Hz, 6H). ESMS m/z 571.2 (M + H^+). HRMS for $C_{30}H_{39}ClN_4O_3S$; calcd: 571.2504, found: 571.2502.

Synthesis of 5-chloro-N2-(2-*iso*-propoxy-5-methyl-4-(1-methylpiperidin-4-yl)phenyl)-N4-(2-(*iso*-propylsulfonyl)phenyl)pyrimidine-2,4-diamine (**16a**)

5-chloro-N2-(2-*iso*-propoxy-5-methyl-4-(1-methylpiperidin-4-yl)phenyl)-N4-(2-(*iso*-propylsulfonyl)phenyl)pyrimidine-2,4-diamine (**16a**) was synthesized according to the same procedure described for **15b** from 71.4 mg (0.2 mmol) **9a** and 160.9 mg (0.614 mmol) of **13d** in 93% overall yield (106.6 mg, 0.187 mmol). ^{1}H NMR (HCl salt, DMSO-*d*6 + trace D_2O): δ 8.28 (s, 1H), 8.19 (d, 1H), 7.86 (d, 1H), 7.66 (dd, 1H), 7.45 (dd, 1H), 7.37 (s, 1H), 6.77 (s, 1H), 4.56-4.49 (m, 1H), 3.51-3.37 (m, 3H), 3.16-3.08 (m, 2H), 2.98-2.88 (m, 1H), 2.77 (s, 3H), 2.05 (s, 3H), 1.90-1.81 (m, 4H), 1.19 (d, 6H), 1.11 (d, 6H). ESMS (m/z: 572.24 $(M+1)^+$. HRMS for $C_{29}H_{38}ClN_5O_3S$; calcd: 572.2457, found: 572.2462.

Synthesis of 5-chloro-N2-(2-*iso*-propoxy-5-methyl-4-(1-ethylpiperidin-4-yl)phenyl)-N4-(2-(*iso*-propylsulfonyl)phenyl)pyrimidine-2,4-diamine (**17a**)

To a solution of **15b** (56 mg, 0.1 mmol) and DIEA (35 uL, 0.2 mmol, 2 eq.) in 3.0 mL of EtOH was added 1-iodoethane (20 mg, 0.13 mmol, 1.3 eq.). The resulting mixture was heated at 50^{o}C overnight. After cooling down to room temperature the reaction mixture was concentrated and the residue was purified by silica column chromatography (eluted with 0-5% MeOH in DCM) to afford 30 mg (0.051 mmol, 51% yield) of **17a**. ^{1}H NMR ($CDCl_3$, 400 MHz) δ 9.51 (s, 1H), 8.58-8.60 (d, J = 8.0 Hz, 1H), 8.18 (s, 1H), 8.06 (s, 1H), 7.94-7.96 (dd, J = 8.0, 1.6 Hz, 1H), 7.62-7.67 (m, 1H), 7.61 (s, 1H), 7.25-7.29 (m, 1H), 7.02 (s, 1H), 4.73-4.76 (m, 1H), 3.60-3.80 (m, 2H), 3.23-3.30 (m, 1H), 3.08-3.18 (m, 2H), 2.98-3.08 (m, 1H), 2.72-2.92 (m, 4H), 2.15 (s, 3H), 1.90-2.05 (m, 2H), 1.57-1.61 (t, J = 8.0 Hz, 3H),1.38-1.40 (d, J = 8.0 Hz, 6H), 1.31-1.33 (d, J = 8.0 Hz, 6H). MS (ES+): 586.26 $(M+1)^{+}$. HRMS for $C_{30}H_{40}ClN_5O_3S$; calcd: 586.2613, found: 586.2620.

Synthesis of 5-chloro-N2-(2-*iso*-propoxy-5-methyl-4-(1-*iso*-propylpiperidin-4-yl)phenyl)-N4-(2-(*iso*-propylsulfonyl)phenyl)pyrimidine-2,4-diamine (**17b**)

17b was synthesized according to the procedure described for **17a** using 56.0 mg (0.1 mmol) of **15b** and 2-iodopropane (22.0 mg, 0.13 mmol) as alkylating agent in overall 37% yield (22.0 mg , 0.0367 mmol). ^{1}H NMR ($CDCl_3$, 400 MHz) δ 9.49 (s, 1H), 8.57-8.59 (d, J = 8.0 Hz, 1H), 8.16 (s, 1H), 8.06 (s, 1H), 7.91-7.94 (dd, J = 8.0, 1.6 Hz, 1H), 7.59-7.65 (m, 3H), 7.23-7.28 (m, 1H), 7.11 (s, 1H), 4.78-4.81 (m, 1H), 3.58-3.60 (m, 3H), 3.23-3.28 (m, 1H), 2.90-3.10 (m, 5H), 2.15 (s, 3H), 1.90-2.00 (m, 2H), 1.53-1.54 (d, J = 4.0 Hz, 6H),1.39-1.40 (d, J = 4.0 Hz, 6H), 1.31-1.32 (d, J = 4.0 Hz, 6H). MS (ES+): 600.2 $(M+1)^{+}$. HRMS for $C_{31}H_{42}ClN_5O_3S$; calcd: 600.2770, found: 600.2777.

Synthesis of 2-[4-(4-{5-Chloro-4-[2-(propane-2-sulfonyl)-phenylamino]-pyrimidin-2-ylamino}-5-*iso*-propoxy-2-methyl-phenyl)-piperidin-1-yl]-ethanol (**17c**)

17c was synthesized in overall 31% yield (22.2 mg , 0.037 mmol) according to the procedure described for **17a** using 75 mg (0.119 mmol) of **15b** and 149 mg (84 μL, 1.19 mmol) of 1-chloro-2-hydroxyethane as alkylating agent: ^{1}H NMR (HCl salt, DMSO-*d*6 + trace D_2O): δ 8.34-8.23 (m, 2H), 7.85 (d, 1H), 7.64 (dd, 1H), 7.47-7.38 (m, 2H), 6.78 (s, 1H), 4.55-4.46 (m, 1H), 3.79-3.72 (m, 2H), 3.63-3.53 (m, 2H), 3.47-3.34 (m, 1H), 3.21-3.03 (m, 4H), 3.02-2.91 (m, 1H), 2.09 (s, 3H), 2.01-1.79 (m, 4H), 1.21 (d, 6H), 1.13 (d, 6H). MS (ES+): 602.3 $(M+1)^+$. HRMS for $C_{30}H_{40}ClN_5O_4S$; calcd: 602.2563, found: 602.2559.

Synthesis of 5-chloro-N2-(2-*iso*-propoxy-4-(1-(2-methoxyethyl)piperidin-4-yl)-5-methylphenyl)-N4-(2-(*iso*-propylsulfonyl)phenyl)pyrimidine-2,4-diamine (**17d**)

17d was synthesized according to the procedure described for **16a** using 37 mg (0.0586 mmol) of **15b** and 8.1 mg (5.5 mL, 0.059 mmol) of 1-chloro-2-methoxyethane as alkylating agent in overall 32% yield (12.0 mg, 0.019 mmol). ^{1}H NMR (HCl salt, DMSO-*d*6 + trace D_2O): δ 8.34-8.28 (m, 1H), 8.25 (s, 1H), 7.85 (d, 1H), 7.63 (dd, 1H), 7.46-7.38 (m, 2H), 6.77 (s, 1H), 4.50 (hept, 1H), 3.70-3.63 (m, 2H), 3.60-3.51 (m, 2H), 3.45-3.23 (m, 2H), 3.32 (s, 3H), 3.14-2.90 (m, 4H), 2.09 (s, 3H), 1.97-1.81 (m, 4H), 1.21 (d, 6H), 1.12 (d, 6H). MS (ES+): 616.3 $(M+1)^+$. HRMS for $C_{31}H_{42}ClN_5O_4S$; calcd: 616.2719, found: 616.2716.

Synthesis of 5-chloro-N2-(2-*iso*-propoxy-5-methyl-4-(1-(1-methylpiperidin-4-yl)piperidin-4-yl)phenyl)-N4-(2-(*iso*-propylsulfonyl)phenyl)pyrimidine-2,4-diamine (**17e**)

5-Chloro-N2-(2-*iso*-propoxy-5-methyl-4-piperidin-4-yl-phenyl)-N4-[2-(propane-2-sulfonyl)-phenyl]-pyrimidine-2,4-diamine **15b** (20 mg, 0.036 mmol) and N-Methyl-4-piperidone (40 mg, 0.36 mmol, 10 eq.) were dissolved in 1,2-dichloroethane (0.3 mL). $NaBH(OAc)_3$ (110 mg, 0.53 mmol, 15 eq.) was added followed by AcOH (4 μL, 0.072 mmol, 2 eq.). This reaction mixture was stirred at room temperature for 3 days. The crude product mixture was diluted with EtOAc and washed with aqueous 1 N NaOH. The organic layer was dried over Na_2SO_4, filtered and concentrated. Purification with preparative RP-HPLC generated **17e** in 19% yield, which was then converted to its HCl salt with 1N HCl in Et_2O. ^{1}H NMR (HCl salt, DMSO-*d*6 + trace D_2O): δ 8.31-8.23 (m, 2H), 7.86 (d, 1H), 7.72-7.62 (m, 2H), 7.47-7.40 (m, 1H), 6.80 (s, 1H), 4.51 (hept, 1H), 3.62-3.37 (m, 6H), 3.22-3.11 (m, 2H), 3.09-2.96 (m, 3H), 2.77 (s, 3H), 2.37-2.28 (m, 2H), 2.09 (s, 3H), 2.09-1.87 (m, 6H), 1.21 (d, 6H), 1.12 (d, 6H). MS (ES+): 655.3 $(M+1)^+$.

Synthesis of 5-chloro-N2-(4-(1-(2,2-difluoroethyl)piperidin-4-yl)-2-*iso*-propoxy-5-methylphenyl)-N4-(2-(*iso*-propylsulfonyl)phenyl)pyrimidine-2,4-diamine (**17f**)

17f was synthesized in 5% yield (3 mg isolated, 0.048 mmol) according to the procedure described for **17a** using **15b** (56 mg, 0.1 mmol) and 2-bromo-1,1-difluoroethane (15 mg, 0.1 mmol) as alkylating agent. δ ^{1}H NMR (400 MHz, $CDCl_3$) δ 8.20 (dd, J = 8.4, 1.2 , 1H), 7.95 (s, 1H), 7.84 (dd, J = 7.6, 2, 1H), 7.24-7.31 (m, 3H), 6.78 (s, 1H), 6.61 (tt, J =53, 3.6, 1H), 4.45 (m, 1H), 3.82 (d, J = 11.6, 2H), 3.40-3.48 (m, 2H), 2.88-3.13 (m, 4H), 2.15-2.25 (m, 2H), 2.14 (s, 3H), 1.90 (d, J = 12.7, 2H), 1.27 (d, J = 6.0, 6H), 1.18 (d, J = 6.8, 6H). MS (ES+): 622.10 $(M+1)^+$. HRMS for $C_{30}H_{38}ClF_2N_5O_3S$; calcd: 622.2425, found: 622.2438.

Synthesis of 2-(4-(4-((5-chloro-4-((2-(*iso*-propylsulfonyl)phenyl)amino)pyrimidin-2-yl)amino)-5-*iso*-propoxy-2-methylphenyl)piperidin-1-yl)acetic acid (**17g**)

17g was synthesized in overall 53% yield (29.5 mg , 0.0479 mmol) according to the procedure described for **17a** using 63 mg (0.09 mmol) of **15b** di-HCl salt and 19 mg (15 μL) of *tert*-butyl 2-chloroacetate as alkylating agent and Boc deprotection (TFA/DCM). ^{1}H NMR (HCl salt, DMSO-*d*6 + trace D_2O): δ 8.29-8.22 (m, 2H), 7.85 (d, 1H), 7.65 (dd, 1H), 7.45-7.38 (m, 2H), 6.79 (s, 1H), 4.57-4.45 (m, 1H), 4.10 (s, 2H), 3.65-3.53 (m, 2H), 3.45-3.33 (m, 1H), 3.22-3.08 (m, 2H), 3.01-2.89 (m, 1H), 2.08 (s, 3H), 2.03-1.80 (m, 4H), 1.21 (d, 6H), 1.12 (d, 6H). MS (ES+): 616.2 $(M+1)^+$. HRMS for $C_{30}H_{38}ClN_5O_5S$; calcd: 616.2355, found: 616.2353.

Synthesis of 2-(4-(4-((5-chloro-4-((2-(*iso*-propylsulfonyl)phenyl)amino)pyrimidin-2-yl)amino)-5-*iso*-propoxy-2-methylphenyl)piperidin-1-yl)acetamide (**17h**)

17h was synthesized in overall 67% yield (41.2 mg , 0.67 mmol) according to the procedure described for **17a** using the HCl salt of **15b** (63 mg, 0.1 mmol) and 18 mg (0.13 mL) of 2-bromoacetamide as alkylating agent. ^{1}H NMR (HCl salt, DMSO-*d*6 + trace D_2O): δ 8.26 (s, 1H), 8.24-8.17 (m, 1H), 7.85 (d, 1H), 7.64 (dd, 1H), 7.43 (dd, 1H), 7.38 (s, 1H), 6.79 (s, 1H), 4.50 (hept, 1H), 3.86 (s, 2H), 3.56-3.48 (m, 2H), 3.43-3.31 (m, 1H), 3.19-3.06 (m, 2H), 2.99-2.88 (m, 1H), 2.05 (s, 3H), 2.05-1.90 (m, 2H), 1.88-1.78 (m, 2H), 1.20 (d, 6H), 1.10 (d, 6H). MS (ES+): 615.2 $(M+1)^+$. HRMS for $C_{30}H_{39}ClN_6O_4S$; calcd: 615.2515, found: 615.2514.

Synthesis of 1-(4-(4-((5-chloro-4-((2-(*iso*-propylsulfonyl)phenyl)amino)pyrimidin-2-yl)amino)-5-*iso*-propoxy-2-methylphenyl)piperidin-1-yl)-2-(dimethylamino)ethanone (**17i**)

5-Chloro-N2-(2-*iso*-propoxy-5-methyl-4-piperidin-4-yl-phenyl)-N4-[2-(propane-2-sulfonyl)-phenyl]-pyrimidine-2, 4-diamine (**15b**, 0.1 mmol) was dissolved in anhydrous DMF (5 mL). Dimethylaminoacetyl chloride hydrochloride (0.15 mmol, 1.5 eq.) was added followed by Et_3N (0.3 mmol, 3 eq.). The reaction mixture was stirred at 25°C for 12 h. After concentration, the crude product was purified using preparative RP-HPLC to give 1-(4-(4-((5-chloro-4-((2-(*iso*-propylsulfonyl)phenyl)amino)pyrimidin-2-yl)amino)-5-*iso*-propoxy-2-methylphenyl)piperidin-1-yl)-2-(dimethylamino)ethanone **17i** as an oil in 70% yield.

^{1}H NMR (400 MHz, CD_3OD) δ 8.46 (d, J = 8.4, 1H), 8.13 (d, J = 2.0, 1H), 7.92 (d, J = 8.0, 1H), 7.77 (s, 1H), 7.66 (t, J = 7.9, 1H), 7.36 (t, J = 7.7, 1H), 6.79 (s, 1H), 4.67 (d, J = 13.1, 1H), 4.57 (dt, J = 6.0, 12.1, 1H), 4.16 (d, J = 13.3, 1H), 3.32 (dt, J = 10.2, 14.1, 3H), 3.20 (dd, J = 10.7, 23.2, 1H), 3.00 (t, J = 11.9, 1H), 2.75 (t, J = 12.3, 1H), 2.35 (s, 6H), 2.16 (s, 3H), 1.80 (d, J = 12.7, 2H), 1.75 – 1.47 (m, 2H), 1.31 (d, J = 6.0, 6H), 1.25 (d, J = 6.8, 6H). MS (ES+): 643.2 $(M+1)^+$. HRMS for $C_{32}H_{43}ClN_6O_3S$; calcd: 643.2828, found: 643.2823.

Synthesis of N2-(2-*iso*-propoxy-5-methyl-4-(1-methylpiperidin-4-yl)phenyl)-N4-(2-(*iso*-propylsulfonyl)phenyl)-5-methylpyrimidine-2,4-diamine (**18a**)

18a was synthesized in overall 19% yield (168 mg , 0.058 mmol) according to the procedure described for **15a** using intermediates **9b** (99.0 mg, 0.305 mmol) and **13d** (80.0 mg, 0.305 mmol)**.** ^{1}H NMR δ (HCl salt, DMSO-*d*6 + trace D_2O, 400 MHz) 8.04 (s, 1H), 7.96 (dd, J = 8.0, 1.6 Hz, 2H), 7.79 (m, 1H), 7.61 (m, 1H), 7.27 (s, 1H), 6.81 (s, 1H), 4.55 (m, 1H), 3.43 (m, 3H), 3.08 (m, 2H), 2.91 (m, 1H), 2.77 (s, 3H), 2.17 (s, 3H), 1.98 (s, 3H), 1.91 (m, 2H), 1.80 (m, 2H), 1.24 (d, J = 6.0 Hz, 6H), 1.10 (d, J = 6.8 Hz, 6H). HRMS for $C_{30}H_{41}N_5O_3S$: calcd: 552.3003, found: 552.3009.

Synthesis of N2-(2-*iso*-propoxy-5-methyl-4-(1-ethylpiperidin-4-yl)phenyl)-N4-(2-(*iso*-propylsulfonyl)phenyl)-5-methylpyrimidine-2,4-diamine (**18b**)

18b was synthesized in overall 28% yield (10.0 mg isolated, 0.014 mmol) according to the procedure described for **17a** using 26.9 mg (0.05 mmol) of intermediate **15c** and 31.2 mg (16.0 µL, 0.2 mmol) 1-iodoethane as alkylating agent. ^{1}H NMR (TFA salt, 400 MHz, CD_3OD) δ 8.28 (s, 1H), 8.01 (dd, J = 1.4, 8.0 Hz, 1H), 7.82 (s, 1H), 7.74 (t, J = 7.5 Hz, 1H), 7.54 (t, J = 7.7 Hz, 1H), 7.35 (s, 1H), 6.89 (s,1H), 4.69 – 4.58 (m, 1H), 3.75 – 3.66 (m, 2H), 3.40 – 3.33 (m, 2H), 3.25 (q, J = 7.3 Hz, 2H), 3.20 – 3.09 (m, 3H), 2.26 (s, 3H), 2.20 (s, 3H), 2.13 –1.91 (m, 4H), 1.41 (t, J = 7.3 Hz, 3H), 1.29 (d, J = 6.0 Hz, 6H), 1.23 (d, J = 6.8 Hz, 6H). MS (ES+): 566.3.

Synthesis of 2-(4-(5-*iso*-propoxy-4-((4-((2-(*iso*-propylsulfonyl)phenyl)amino)-5-methylpyrimidin-2-yl)amino)-2-methylphenyl)piperidin-1-yl)ethanol (**18c**)

18c was synthesized in overall 36% yield (21 mg isolated, 0.036 mmol) according to the procedure described for **17a** using 54 mg (0.10 mmol) intermediate **15c** and 62 mg (0.50 mmol) 1-bromo-2-hydroxyethane as alkylating agent: ^{1}H NMR (400 MHz, CD_3OD) δ 8.50 (d, J = 8.0, 1H), 7.93 (s, 1H), 7.89 (d, J = 8.0, 1H), 7.84 (s, 1H), 7.66 (t, J = 7.1, 1H), 7.31 (t, J = 7.2, 1H), 6.85 (s, 1H), 4.66 – 4.54 (m, 1H), 3.74 (t, J = 6.2, 2H), 3.12 (d, J = 11.6, 2H), 2.73 (m, 1H), 2.60 (t, J = 6.1, 2H), 2.23 (m, 3H), 2.17 (d, J = 7.6, 3H), 2.11 (s, 3H), 1.76 (m, 4H), 1.33 (dd, J = 6.0, 11.1, 6H), 1.24 (d, J = 6.8, 6H). MS (ES+): 582.2. HRMS for $C_{31}H_{43}N_5O_4S$; calcd: 582.3109, found: 582.3104.

Synthesis of N2-(2-*iso*-propoxy-4-(1-(2-methoxyethyl)piperidin-4-yl)-5-methylphenyl)-N4-(2-(*iso*-propylsulfonyl)phenyl)-5-methylpyrimidine-2,4-diamine (**18d**)

18d was synthesized in 36% yield (21 mg isolated, 0.036 mmol) according to the procedure described for **17a** using intermediate **15c** (54 mg, 0.1 mmol) and 1-chloro-2-methoxyethane (62 mg, 0.5 mmol) as alkylating agent. ^{1}H NMR (400 MHz, CD_3OD) δ 8.29 (s, 1H), 8.01 (d, J = 8.0, 1H), 7.82 (s, 1H), 7.73 (t, J = 7.8, 1H), 7.54 (t, J = 7.7, 1H), 7.32 (s, 1H), 6.91 (s, 1H), 4.64 (dt, J = 6.0, 12.1, 1H), 3.79 – 3.74 (m, 3H), 3.73 (s, 1H), 3.44 (m, 3H), 3.40 (m, 2H), 3.16 (m, 4H), 2.25 (s, 3H), 2.20 (s, 3H), 2.03 (m, 4H), 1.29 (d, J = 6.0, 6H), 1.23 (d, J = 6.8, 6H). MS (ES+): 596.3. HRMS for $C_{32}H_{45}N_5O_4S$; calcd: 596.3265, found: 596.3273.

Synthesis of Synthesis of 2-((5-chloro-2-((2-*iso*-propoxy-5-methyl-4-(1-methylpiperidin-4-yl)phenyl)amino)pyrimidin-4-yl)amino)-N,N-dimethylbenzenesulfonamide (**16b**)

16b was synthesized according to the same procedure described for **15a** from 34.4 mg (0.1 mmol) of **9d** and 26.2 mg (0.1 mmol) of **13d** in overall 25% yield (14.5 mg, 0.025 mmol). ^{1}H NMR δ (HCl salt, CD_3OD, 400 MHz) 8.14 (s, 1H), 8.09 (broad s, 1H), 7.87 (dd, J = 8.0, 1.6 Hz, 1H), 7.60 (m, 1H), 7.44 (m, 1H), 7.25 (s, 1H), 6.84 (s, 1H), 4.59 (m, 1H), 3.53 (m, 2H), 3.14 (m, 2H), 3.03 (m, 1H), 2.83 (s, 3H), 2.62 (s, 6H), 1.92 (m, 4H), 1.20 (d, J = 6.0 Hz, 6H). MS (ES+): 573.3. HRMS for $C_{28}H_{37}ClN_6O_3S$; calcd: 573.2409, found: 573.2426.

Synthesis of 4-(4-((5-chloro-4-((2-(*iso*-propylsulfonyl)phenyl)amino)pyrimidin-2-yl)amino)-5-*iso*-propoxy-2-methylphenyl)piperidin-2-one (**19**)

To a mixture of 2,5-dichloro-N-(2-(*iso*-propylsulfonyl)phenyl)pyrimidin-4-amine **9a** (34.5 mg, 0.10 mmol, 1 eq.) and 2-*iso*-propoxy-5-methyl-4-(2-oxopiperidin-4-yl)benzenaminium 2,2,2-

trifluoroacetate **13e** (37.6 mg, 0.10 mmol, 1 eq.) in 2-propanol (1.0 mL) was added concentrated HCl (40 uL, 5 eq.). The 5 mL microwave reaction vessel was then sealed and heated under microwave irradiation to 150°C for 30 minutes followed by purification with preparative RP-HPLC to give 2.0 mg (0.0035 mmol, 3.5%) of 4-(4-((5-chloro-4-((2-(iso-propylsulfonyl)phenyl)amino)pyrimidin-2-yl)amino)-5-iso-propoxy-2-methylphenyl)piperidin-2-one (**19**). ^{1}H NMR δ (TFA salt, DMSO-*d*6, 400 MHz) 9.50 (s, 1H), 8.44 (d, J = 8.4 Hz, 1H), 8.27 (s, 1H), 8.15 (s, 1H), 7.84 (dd, J = 8.0, 1.6 Hz, 1H), 7.65 (m, 1H), 7.60 (m, 1H), 7.52 (s, 1H), 7.38 (m, 1H), 6.91 (s, 1H), 4.59 (m, 1H), 3.45 (m, 1H), 3.22 (m, 3H), 2.31 (m, 2H), 2.13 (s, 3H), 1.82 (m, 2H), 1.22 (d, J = 6.0 Hz, 6H), 1.16 (d, J = 6.0 Hz, 6H). MS (ES+): 572.1. HRMS for $C_{28}H_{34}ClN_5O_4S$; calcd: 572.2093, found: 572.2106.

Synthesis of 5-chloro-N2-(4-*iso*-propoxy-2-(piperidin-4-yl)pyrimidin-5-yl)-N4-(2-(*iso*-propylsulfonyl)phenyl)pyrimidine-2,4-diamine (**20**)

20 was synthesized in overall 27% yield (6.6 mg isolated, 0.012 mmol) according to the procedure described for **15b** using **9a** (17.0 mg, 0.05 mmol) and 4-(5-amino-4-*iso*-propoxy-4-*iso*-propoxypyrimidin-2-yl)-piperidine-1-carboxylic acid *tert*-butyl ester (10 mg, 0.0.297 mmol) **13f** as reagents. ^{1}H NMR (CD_3OD, 400 MHz) δ 9.04 (s, 1H), 8.45-8.47 (d, J = 8.0 Hz, 1H), 8.25 (s, 1H), 7.92-7.95 (dd, J = 8.0, 1.6 Hz, 1H), 7.71-7.75 (m, 1H), 7.38-7.42 (m, 1H), 5.52-5.55 (m, 1H), 3.50-3.53 (m, 3H), 3.10-3.18 (m, 3H), 2.24-2.26 (m, 2H), 2.02-2.16 (m, 2H), 1.41-1.43 (d, J = 6 Hz, 6H), 1.25-1.27 (d, J =6.8 Hz, 6H). MS (ES+): 546.20.

Cell lines

The murine pro-B cell line Ba/F3, human cell line Karpas-299 were maintained in RPMI medium 1640 supplemented with 10% FBS. Ba/F3 cells were grown in the presence of IL-3 (10 ng/ml). Ba/F3 cells were used to generate a panel of sublines whose proliferation and survival was rendered IL-3-independent by stable transduction with individual tyrosine kinases activated by fusion with the amino-terminal portion of TEL (amino acid 1-375), or with BCR-Abl, NPM-ALK, or EML4-ALK. Cell lines expressing luciferase alone or in combination with fusion constructs were generated by retroviral transduction of cells with pMSCV IRES puro/Luc vector.

Cell Proliferation Assays.

Luciferase-expressing cells were incubated with serial dilutions of compounds or DMSO for 2–3 days. Luciferase expression was used as a measure of cell proliferation/survival and was evaluated with the Bright-Glo Luciferase Assay System (Promega, Madison, WI). IC50 values were generated by using XLFit software.

Enzymatic kinase profiling description.

All kinases were expressed as either Histidine- or GST-tagged fusion proteins using the baculovirus expression technology except for the untagged ERK2 which was produced in E. coli. AURORA-A, JAK2, MK2, SYK and PKA were purchased from Invitrogen, ERK2 from ProQinase and all other kinases were supplied in-house. The kinase activity was measured in the LabChip mobility-shift assay (PerkinElmer). The assay was performed at 30°C for 60 min.

The effect of compound on the enzymatic activity was obtained from the linear progress curves in the absence and presence of compound and routinely determined from one reading (end point measurement).

GSH-trapping assay

For the characterization of the metabolic activation, 10 mmol/L DMSO stock solutions the compounds were incubated at 37 ºC for up to 60 minutes with human liver microsomes (50 µL), containing 1 mg protein/mL with phosphate buffer. Four microliters of a 0.5 mM of 20 µL DMSO stock solution of compound in 180 µL of a mixture of acetonitrile/water (ratio 1:1) was added to 50 µL of 1 mg/mL of liver microsomes in phosphate buffer and pre-incubated for 3 min at 37 °C. After pre-incubation, the reaction was started by addition of 50 µL of the NADPH (1 mmol/L), UDPGA (1 mmol/L), MgCl (2 mmol/L) and ethylester GSH reduced (2 mmol/L). After 60 min, the reaction was stopped with 200 µL ice-cold acetonitrile. The reaction mixture was stored at -20 °C. The mixture was centrifuged (10000 g, 5 min) and 250 µL of 300 µL supernatant was transferred. From this solution, 20 µL aliquots were used for analysis. The liquid chromatographic separation was performed using an Agilent HP1100 pump (Agilent Technologies, Wilmington, DE) and a Phenyl HexylRP column, 150 mm x 2.0 mm, particle size 4.6 µm. Gradient mobile phase programming was used with a flow rate of 350 µL/min. Eluent A was Milli-Q water with 0.1% formic acid. Eluent B was acetonitrile with 0.1% formic acid. The mobile phase was a linear gradient from 5% B to 95% B over 6 min and held for 2 min at 95% B for a total run time of 10 minutes. The column effluent was introduced directly into the ion source of a triple quadrupole MS (TS-Quantum, Finnigan, San Jose, CA) or ion trap MS (DecaXP, Finnigan, San Jose, CA). The ionization technique employed was positive electrospray (ES). The Quantum was used in a product ion scan mode, utilizing collision induced dissociation in Q2 (collision chamber). Collision gas was argon. The collision energy was set at 30 eV.

Solubility assays

One hundred microliter aliquots of 1 mM DMSO solutions were added to each of three glass vials and evaporated to dryness prior to addition of 500 μL of pH 6.8 buffer. Following 24h shaking, the solutions were vacuum filtered through MultiScreen Solubility 96 well plates with 0.4 μm modified PCTE membrane (Millipore, MSSLBPC10) and an aliquot of each filtrate is transferred to a UV plate for quantification as described in Uvarova *et al*.[46]

Metabolic Clearance assays.

The metabolic clearance assays were conducted using the method described in Richmond, *et al*.[44]

CYP inhibition assays.

The samples were prepared as 10 mM solutions in DMSO, then assayed and analyzed using the general LC/MS/MS method described by Bell, *et al*.[47]

PK studies

In vivo PK studies were conducted in mice, rats, dogs and Cynomolgus monkeys. **15b** (HCl salt) was formulated as a solution in 75% PEG300/25% D5W and administered to male Balb/c mice intravenously via tail vein at 5 mg/kg (n=3) and orally via gavage at 20 mg/kg (n=3). Using the same formulation, **15b** (HCl salt) was dosed to Sprague Dawley rats intravenously via the tail vein at 3 mg/kg (n=3) and orally via gavage at 10 mg/kg (n=3). Blood samples were collected serially at scheduled times over 24 hours after dosing.

Male beagle dogs received single intravenous (n=2) or oral (n=3) dose of **15b** (phosphate salt) as an intravenous solution in 30% propylene glycol/5% Solutol® buffer at 5 mg/kg and an oral suspension in suspension in 0.5% (w/v) aqueous methylcellulose /0.5% Tween 80 at 20 mg/kg, respectively.

Male Cynomologus monkeys received single intravenous (n=2) or oral (n=3) dose of **15b** (free base) as an intravenous solution in 30% propylene glycol/5% solutol at 5 mg/kg and an oral suspension in 0.5% (w/v) methylcellulose at 60 mg/kg, respectively. Blood samples for plasma were collected at pre-scheduled times over 144 hours after dosing.

In Vivo Experiments.

RNU nude rats bearing the Karpas299 tumors were randomized into 5 groups (n=6 rats per group) with an average tumor size of 326 ± 128 mm^3. **15b** (phosphate salt) was formulated in 0.5% MC/0.5% Tween 80 and administered by oral gavage at a dosing volume of 10 μL/g of an animal body weight. Animals in each group received vehicle or 6.25, 12.5, 25, 50 mg/kg **15b** every day for 14 consecutive days.

RNU nude rats bearing the H2228 tumors were randomized into 4 groups (n=4 rats per group) with an average tumor volume of 371 ± 139 mm^3. **15b** (phosphate salt) was formulated in 0.5% MC / 0.5% Tween 80 and administered by oral gavage at a dosing volume of 10 μL/g of an animal body weight. Animals in each group received vehicle or 5, 10, 25 mg/kg **15b** (phosphate salt) every day for 14 consecutive days.

RNU nude rats bearing the Karpas299 tumors were dosed with **15b** (phosphate salt) at 50 mg/kg. Tumor and plasma samples were collected 7, 24, 48 and 72 hours after dosing. 2 tumor pieces were collected from each animal, one piece for protein extraction and the other for PK

analysis. Proteins were extracted from tumor samples and then subjected to SDS-PAGE followed by western blot with phospho-STAT3 antibody (pSTAT3, Tyr705) (Cell Signaling, #9131, Danvers, MA).

HOMA-IR

Homeostatic model assessment (HOMA) of insulin resistance (IR) is a technical method for assessing IR from basal (fasting) glucose and insulin or C-peptide concentrations. The model is widely used to estimate insulin resistance.[48]

Groups of wild-type mice (n=8 mice per group) were randomized into treatment groups based on their initial body weight. Mice were housed four per cage and dosed with vehicle orally, or ALK inhibitor (**15b** or **4**), orally once per day for seven days. On Day 7, compound was administered 180 minutes prior to a 3 g/kg glucose bolus. OGTT evaluations were performed in conscious mice that were 11 weeks of age. The mice were fasted by removing food at 6 p.m. the day before. A baseline blood sample was taken at t = - 180 minutes and the mice were then dosed orally with the compounds. A baseline blood sample was taken at t = 0 minutes and the animals were then administered an oral glucose bolus (3 g/kg) immediately. Blood was obtained (via tail bleeding) to measure blood glucose (using glucometer). A single drop of blood from the tail was measured for glucose using a glucometer at t = -180, 0, 20, 40, 60, 120 minutes. Approximately 40 µL samples of blood were collected separately for insulin analysis 3 hours prior to dosing (on Day 0 and Day 7) into chilled collection tubes containing EDTA. Plasma was isolated and stored at -70°C until further analysis. The homeostatic model assessment–insulin resistance index (HOMA-IR) was used as a measure of insulin resistance and was calculated using the formula: $HOMA\text{-}IR = (FPG * FPI) / 22.5$ where FPG (mM) is the fasting plasma

glucose concentration, FPI (μU/ml) is the fasting plasma insulin concentration. Insulin levels were determined using a detection assay kit from Mesoscale Discovery (MSD): Catalog# K112BZC-2. Higher values indicate insulin resistance.

Modeling and docking

Flexible docking was performed using Glide 5.8 (Schrodinger, Inc, Portland, OR, 2012). The protein coordinates were taken from protein databank (2xb7.pdb). The grid box was centered on the co-crystallized ligand **15b** and extended 10 Å from the center, with outer box extending an additional 20 A. The ligand was docked using the standard precision (SP) algorithm and scored using GlideScore.

In MCMM/LLMOD method the structural perturbation via LLMOD method is alternated with the random changes in torsion angles and/or molecular position from MCMM method. During the LLMOD structural perturbation and subsequent minimization, protein residues within 4 Å from the bound ligand were allowed to move freely. The remaining residues were not allowed to move, however their electrostatic and van der Waals interactions with moving atoms was included in the calculation. The inhibitor was subjected to perturbations via TORS command available in MacroModel. The LLMOD step was applied using a leap vectors comprised of different random mixtures of the first 10 nontrivial low-modes and the fastest-moving atom with respect to the particular leap vector was displaced by a randomly selected distance between 3 - 6 Å. During the TORS move randomly selected torsion angle was perturbed by a random value between 0 – 180°. A conjugate gradient minimization was employed during the conformational

search with convergence criteria set at 0.5 kJ/mol Å. Minimum energy conformations were saved within an energy window of 40 kJ/mol above the global minimum. The employed force field was OPLS-AA 2005 with distance dependent dielectric constant 4r and no explicit solvation.

AUTHOR ADDRESS. Genomics Institute of the Novartis Research Foundation, 10675 John Jay Hopkins Drive, San Diego, CA 92121. * To whom correspondence should be addressed. pmichellys@gnf.org, Tel: (858) 332-4781

ABREVIATIONS: ALK, anaplastic lymphoma kinase; ALKi, anaplastic lymphoma kinase inhibitor; NPM, nucleophosmin; SAR, structure activity relationship; ALCL, anaplastic large cell lymphoma; NSCLC, non-small cell lung cancer; DLBCL, diffuse large B-cell lymphoma; IMT, myofibroblastic tumors; nM, nanomolar; Boc, *tert*-butoxycarbonyl; MW, microwave irradiation, ADME, absorption, distribution, metabolism and excretion; PK, pharmacokinetic;TLC, thin-layer chromatography; GSH, glutathione; HOMA-IR, homeostatic model assessment of insulin resistance.

SUPPORTING INFORMATION AVAILABLE. GSH-trapping results (LC-UV) for **4** anf **15b,** body weight of animals from Karpas299 and H2228 xenograft studies, superposition of compounds **15b** and **16e** in ALK kinase domain and kinase selectivity comparison between **4** and **7**. This material is available free of charge via the internet at http://pubs.acs.org.

ACKNOWLEDGEMENTS: the authors wish to acknowledge Daniel Mason for providing HRMS data on the compounds described in this manuscript, John Isbell (analytical group from GNF) and Paul Calvin and his group (compound management)

REFERENCES

(1) Morris, S. W.; Naeve, C.; Mathew, P.; James, P. L.; Kirstein, M. N.; Cui, X.; Witte, D. P. ALK, the chromosome 2 gene locus altered by the t(2;5) in non-Hodgkin's lymphoma, encodes a

novel neural receptor tyrosine kinase that is highly related to leukocyte tyrosine kinase (LTK). *Oncogene*. 1997, *14*, 2175–2188.

(2) Chiarle, R.; Voena, C.; Ambrogio, C.; Piva, R.; Inghirami, G. The anaplastic lymphoma kinase in the pathogenesis of cancer. *Nature Rev. Cancer.* 2008, *8(1)*, 11-23.

(3) Webb, T. R.; Slavish, J.; George, R. E.; Look, A. T.; Xue, L.; Jiang, Q.; Cui, X.; Rentrop, W. B.; Morris, S. W. Anaplastic lymphoma kinase: role in cancer pathogenesis and small-molecule inhibitor development for therapy. *Expert Rev. Anticancer Ther.* 2009, *9(3)*, 331-356.

(4) Iwahara T.; Fujimoto J.; Wen D.; Cupples R.; Bucay N.; Arakawa T.; Mori S.; Ratzkin B.; Yamamoto T. Molecular characterization of ALK, a receptor tyrosine kinase expressed specifically in the nervous system. *Oncogene*. 1997, *14*, 439-449.

(5) Bilsland J. G.; Wheeldon A.; Mead A.; Znamenskiy P.; Almond S.; Waters K. A.; Thakur M.; Beaumont V.; Bonnert T. P.; Heavens R.; Whiting P.; McAllister G.; Munoz-Sanjuan I. Behavioral and Neurochemical Alterations in Mice Deficient in Anaplastic Lymphoma Kinase Suggest Therapeutic Potential for Psychiatric Indications. *Neuropsychopharmacology*. 2008, *33*, 685–700.

(6) Morris S. W.; Kirstein M. N.; Valentine M. B.; Dittmer K. G.; Shapiro D. N.; Saltman D. L.; Look A. T. Fusion of a kinase gene, ALK, to a nucleolar protein gene, NPM, in non-Hodgkin's lymphoma. *Science*. 1994, *263*, 1281-1284.

(7) Griffin, C. A.; Hawkins, A. L.; Dvorak, C.; Henkle, C.; Ellingham,T.; Perlman, E. J. Recurrent Involvement of 2p23 in Inflammatory Myofibroblastic Tumors. *Cancer Res.* 1999, *59*, 2776–2780.

(8) Soda, M.; Choi, Y. L.; Enomoto, M.; Takada, S.; Yamashita, Y.; Ishikawa, S.; Fujiwara, S.; Watanabe, H.; Kurashina, K.; Hatanaka, H.; Bando, M.; Ohno, S.; Ishikawa, Y.; Aburatani, H.; Niki, T.; Sohara, Y.; Sugiyama, Y.; Mano, H. Identification of the transforming EML4–ALK fusion gene in non-small-cell lung cancer. *Nature*. 2007, *448*, 561–566.

(9) Mano, H. Non-solid oncogenes in solid tumors: EML4–ALK fusion genes in lung cancer. *Cancer Sci.* 2008, *99*, 2349–2355.

(10) Shaw, A. T.; Solomon, B. Targeting Anaplastic Lymphoma Kinase in Lung Cancer. *Clin. Cancer Res*. 2011, *17(8)*, 2081–2086.

(11) Osajima-Hakomori, Y.; Miyake, I.; Ohira, M.; Nakagawara, A.; Nakagawa, A.; Sakai, R. Biological Role of Anaplastic Lymphoma Kinase in Neuroblastoma. *Am. J. Pathol.* 2005, *167*, 213–222.

(12) Mosse, Y. P.; Laudenslager, M.; Longo, L.; Cole, K.A.; Wood, A.; Attiyeh, E. F.; Laquaglia,M. J.; Sennett, R.; Lynch, J. E.; Perri, P.; Laureys, G.; Speleman, F.; Kim, C.; Hou, C.; Hakonarson, H.; Torkamani, A.; Schork, N. J.; Brodeur, G. M.; Tonini, G. P.; Rappaport, E.; Devoto, M.; Maris., J. M. Identification of ALK as a major familial neuroblastoma predisposition gene. *Nature*. 2008, *455*, 930–935.

(13) Azarova, A. M.; Gautam, G.; George, R. E. Emerging importance of ALK in neuroblastoma. *Seminars in Cancer Bio.* 2011, *21*, 267– 275.

(14) Tuma, R. S. ALK Gene Amplified in Most Inflammatory Breast Cancers. *J. Nat. Cancer Inst.* 2012, *104(2)*, 87-88.

(15) Ren, H.; Tan, X. Z.; Crosby, C.; Haack, H.; Ren, J.-M.; Beausoleil, S.; Moritz, A.; Innocenti, G.; Rush, J.; Zhang, Y.; Zhou, X.-M.; Gu, T.-L.; Ynag, Y.-F.; Comb, M. J. Identification of Anaplastic Lymphoma Kinase as a Potential Therapeutic Target in Ovarian Cancer. *Cancer Res.* 2012, *72*, 3312-3323.

(16) Ott, G. R.; Tripathy, R.; Cheng, M.; McHugh, R.; Anzalone, A. V.; Underiner, T. L.; Curry, M. A.; Quail, M. R.; Lu, L.; Wan, W.; Angeles, T. S.; Albom, M. S.; Aimone, L. D.; Ator, M. A.; Ruggeri, B. A.; Dorsey, B. D. Discovery of a Potent Inhibitor of Anaplastic Lymphoma Kinase with in Vivo Antitumor Activity. *ACS Med. Chem. Lett.* 2010, *1*, 493–498.

(17) Mesaros, E. F.; Burke, J. P.; Parrish, J. D.; Dugan, B. J.; Anzalone, A. V.; Angeles, T. S.; Albom, M. S.; Aimone, L. D.; Quail, M. R.; Wan, W.; Lu, L.; Huang, Z.,; Ator, M. A.; Ruggeri, B. A.; Cheng, M.; Ott, G. R.; Dorsey, B, D. Novel 2,3,4,5-tetrahydro-benzo[d]azepine derivatives of 2,4-diaminopyrimidine, selective and orally bioavailable ALK inhibitors with antitumor efficacy in ALCL mouse models. *Bioorg. Med. Chem. Lett.* 2011, *21*, 463–466.

(18) Milkiewicz,K. L; Weinberg, L. R.; Albom, M. S.; Angeles, T. S.; Cheng, M. Synthesis and structure–activity relationships of 1,2,3,4-tetrahydropyrido[2,3-b]pyrazines as potent and selective inhibitors of the anaplastic lymphoma kinase. *Bioorg. Med. Chem.* 2010, *18*, 4351–4362.

(19) Ott, G. R.; Wells, G. J.; Thieu, T. V.; Quail, M. R.; Lisko, G. J.; Mesaros, E. F.; Gingrich, D. E.; Ghose, A. K.; Wan, W.; Lu, L.; Cheng, M.; Albom, M. S.; Angeles, T. S.; Huang, Z.; Aimone, L. D.; Ator, M. A.; Ruggeri, B. A.; Dorsey B. D. 2,7-Disubstituted-pyrrolo[2,1-f][1,2,4]triazines: New Variant of an Old Template and Application to the Discovery of

Anaplastic Lymphoma Kinase (ALK) Inhibitors with in Vivo Antitumor Activity *J. Med. Chem.* 2011, *54(18)*, 6328–6341.

(20) Li, R.; Xue, L.; Zhu, T.; Jiang, Q.; Cui, X.; Yan, Z.; McGee, D.; Wang, J.; Gantla, V. R.; Pickens, J. C.; McGrath, D.; Chucholowski, A.; Morris, S. W.; Webb, T. R. Design and Synthesis of 5-Aryl-pyridone-carboxamides as Inhibitors of Anaplastic Lymphoma Kinase. *J. Med. Chem.* 2006, *49*, 1006-1015.

(21) Ardini, E.; Menichincheri, M.; De Ponti, C.; Amboldi, N.; Ballinari, D.; Saccardo, M. B.; Croci, V.; Stellari, F.; Texido, G.; Orsini, P.; Perrone, E.; Bandiera, T.; Borgia, A. L;, Lansen, J.; Isacchi, A.; Colotta, F.; Pesenti, E.; Magnaghi P.; Galvani, A. A Highly Potent, Selective and Orally Available ALK Inhibitor with Demonstrated Antitumor Efficacy in ALK Dependent Lymphoma and Non-Small Cell Lung Cancer Models. American Association for Cancer Research (AACR) Annual Meeting in San Diego, CA. 2009, abstract #3737.

(22) Sabbatini, P.; Korenchuk, S.; Rowand, J. L.; Groy, A.; Liu,Q.; Leperi, D.; Atkins, C.; Dumble, M.; Yang, J.; Anderson, K.; Kruger, R. G.; Gontarek, R. R.; Maksimchuk, K. R.; Suravajjala, S.; Lapierre, R. R.; Shotwell, J. B.; Wilson, J. W.; Chamberlain, S. D.; Rabindran, S. K.; Kumar, R. GSK1838705A inhibits the insulin-like growth factor-1 receptor and anaplastic lymphoma kinase and shows antitumor activity in experimental models of human cancers. *Mol. Cancer Therapeutics*. 2009, *8(10)*, 2811-2820.

(23) Lewis R. T.; Bode, C. M.; Choquette, D. M.; Potashman, M.; Romero, K.; Stellwagen, J. C.; Teffera, Y.; Moore, E.; Whittington, D. A.; Chen, H.; Epstein, L. F.; Emkey, R.; Andrews, P. S.; Yu, V. L.; Saffran, D. C.; Xu, M.; Drew, A.; Merkel, P.; Szilvassy, S.; Brake, R. L. The Discovery and Optimization of a Novel Class of Potent, Selective, and Orally Bioavailable

Anaplastic Lymphoma Kinase (ALK) Inhibitors with Potential Utility for the Treatment of Cancer. *J. Med. Chem.* 2012, *55*, 6523−6540.

(24) Deng, X.; Wang, J.; Zhang, J.; Sim, T.; Kim, N. D.; Sasaki, T.; Luther, W. II; George, R. E.; Jänne, P. A.; Gray, N. S. Discovery of 3,5-Diamino-1,2,4-triazole Ureas as Potent Anaplastic Lymphoma Kinase Inhibitors. *ACS Med. Chem. Lett.* 2011, *2*, 379–384.

(25) Christensen, J. G.; Zou, H. Y.; Arango, M. E.; Li, Q.; Lee, J. H.; McDonnell, S. R.; Yamazaki, S.; Alton, G. R.; Mroczkowski, B.; Los, G. Cytoreductive antitumor activity of PF-2341066, a novel inhibitor of anaplastic lymphoma kinase and c-Met, in experimental models of anaplastic large-cell lymphoma. *Mol. Cancer Therapeutics*. 2007, *6(12)*, 3314-3322.

(26) Rodig, S. J.; Shapiro, G. I.. Crizotinib, A Small-Molecule Dual Inhibitor of the c-Met and ALK Receptor Tyrosine Kinases. *Curr. Opin. Invest. Drugs.* 2010, *11*, 1477–1490.

(27) Cui, J. J.; Tran-Dube, M.; Shen, H.; Nambu, M.; Kung, P.-P.; Pairish, M.; Jia, L.; Meng, J.; Funk, L.; Botrous, I.; McTigue, M.; Grodsky, N.; Ryan, K.; Padrique, E.; Alton, G.; Timofeevski, S.; Yamazaki, S.; Li, Q.; Zou, H.; Christensen, J.; Mroczkowski, B.; Bender, S.; Kania, R. S.; Edwards. M. P. Structure Based Drug Design of Crizotinib (PF-02341066), a Potent and Selective Dual Inhibitor of Mesenchymal–Epithelial Transition Factor (c-MET) Kinase and Anaplastic Lymphoma Kinase (ALK). *J. Med. Chem.* 2011, *54(18)*, 6342–6363.

(28) Kwak E. L.; Bang Y. J.; Camidge D. R.; Shaw A. T.; Solomon B.; Maki R. G.; Ou S. H.; Dezube B. J.; Jänne P. A.; Costa D. B.; Varella-Garcia M.; Kim W. H.; Lynch T. J.; Fidias P.; Stubbs H.; Engelman J. A.; Sequist L. V.; Tan W.; Gandhi L.; Mino-Kenudson M.; Wei G. C.; Shreeve S. M.; Ratain M. J.; Settleman J.; Christensen J. G.; Haber D. A.; Wilner K.; Salgia R.;

Shapiro G. I.; Clark J. W.; Iafrate A. J. Anaplastic Lymphoma Kinase Inhibition in Non–Small-Cell Lung Cancer. *N. Engl. J. Med.* 2010, *363(18)*, 1693-1703.

(29) Sakamoto, H.; Tsukaguchi, T.; Hiroshima, S.; Kodama, T.; Kobayashi, T.; Fukami, T. A.; Oikawa, N.; Tsukuda, T.; Ishii, N.; Aoki. Y. CH5424802, a Selective ALK Inhibitor Capable of Blocking the Resistant Gatekeeper Mutant. *Cancer Cell*. 2011, *19*, 679–690.

(30). Kinoshita, K.; Kobayashi, T.; Asoh, K.; Furuichi, N.; Ito, T.; Kawada, H.; Hara, S.; Ohwada, J.; Hattori, K.; Miyagi, T.; Hong, W.-S.; Park, M.-J.; Takanashi, K.; Tsukaguchi, T.; Sakamoto, H.; Tsukuda, T.; Oikawa, N. 9-Substituted 6,6-Dimethyl-11-oxo-6,11-dihydro-5H-benzo[b]carbazoles as Highly Selective and Potent Anaplastic Lymphoma Kinase Inhibitors. *J. Med. Chem.* 2011, *54*, 6286–6294.

(31) Kuromitsu, S.; Mori, M.; Shimada, I.; Kondoh Y.; Shindoh N.; Soga T.; Furutani T.; Konagai S.; Sakagami H.; Nakata M.; Ueno Y.; Saito R.; Sasamata M.; Kudou M. Anti-tumor activity of ASP3026, - A novel and selective ALK inhibitor. of Anaplastic Lymphoma Kinase (ALK). American Association for Cancer Research (AACR) Annual Meeting in Orlando, Florida. 2011, abstract #2821.

(32) Lovly, C. M.; Heuckmann, J. M.; De Stanchina, E.; Chen, H.; Thomas, R. K.; Liang, C.; Pao W. Insights into ALK-Driven Cancers Revealed through Development of Novel ALK Tyrosine Kinase Inhibitors. *Cancer Res*. 2011, *71(14)*, 4920-4931.

(33) Katayama, R.; Khan, T. M.; Benes, C.; Lifshits, E.; Eb, H.; River, V. M.; Shakespeare, W. C.; Iafrate, A. J.; Jeffrey A. Engelman; J. A., Shaw, A. T. Therapeutic strategies to overcome crizotinib resistance in non-small cell lung cancers harboring the fusion oncogene EML4-ALK. *Proceed. Nat. Acad. Sci. USA*. 2011, *108(18)*, 7535–7540.

(34) Rivera, V. M.; Anjum, R.; Wang, F.; Zhang, S.; Keats, J.; Ning, Y.; Wardwell, S. D.; Moran, L.; Ye, E.; Chun, D. Y.; Mohemmad, K. Q.; Liu, S.; Huang, W.-S.; Wang, Y.; Thomas, M.; Li, F.; Qi, J.; Miret, J.; Iuliucci, J. D.; Dalgarno, D.; Narasimhan, N. I.; Clackson, T.; Shakespeare, W. C. Efficacy and pharmacodynamic analysis of AP26113, a potent and selective orally active inhibitor of Anaplastic Lymphoma Kinase (ALK). American Association for Cancer Research (AACR) Annual Meeting in Washington, D.C., 2010, abstract #3623.

(35) a.) Li, N.; Michellys, P.-Y.; Kim, S.; Pferdekamper, A. C.; Li, J.; Kasibhatla, S.; Tompkins, C. S.; Steffy, A.; Li, A.; Sun, F.; Sun, X.; Hua, S.; Tiedt, R.; Sarkisova, Y.; Marsilje, T. H.; McNamara, P.; Harris, J. Activity of a potent and selective phase I ALK inhibitor LDK378 in naive and crizotinib-resistant preclinical tumor models. AACR-NCI-EORTC International Conference: Molecular Targets and Cancer Therapeutics in San Francisco, CA, 2011, abstract # B232. b.) Galkin, A. V.; Melnick, J. S.; Kim, S.; Hood, T. L.; Li, N.; Li, L.; Xia, G.; Steensma, R.; Chopiuk, G.; Jiang, J.; Wan, Y.; Ding, P.; Liu, Y.; Sun, F.; Schultz, P. G.; Gray, N. S.; Warmuth, M. Identification of NVP-TAE684, a potent, selective, and efficacious inhibitor of NPM-ALK. *Proceed. Nat. Acad. Sci. USA*. 2007, *104(1)*, 270–275.

(36) Walker, D. P.; Bi, F. C.; Kalgutkar, A. S.; Bauman, J. N.; Zhao, S. X.; Soglia, J. R.; Aspnes, G. A.; Kung, D. W.; Klug-McLeod, J.; Zawistoski, M. P.; McGlynn, M. A.; Oliver, R.; Dunn, M.; Li, J.-C.; Richter, D. T.; Cooper, B. A.; Kath, J. C.; Hulford, C. A.; Autry, C. L.; Luzzio, M. J.; Ung, E. J.; Roberts, W. G.; Bonnette, P. C.; Buckbinder, L.; Mistry, A.; Griffor, M. C.; Han S.; Guzman-Perez, A. Trifluoromethylpyrimidine-based inhibitors of proline-rich tyrosine kinase 2 (PYK2): Structure–activity relationships and strategies for the elimination of reactive metabolite formation. *Bioorg. Med. Chem. Lett.* 2008, *18*, 6071–6077.

(37) Obach, R. S.; Kalgutkar, A. S.; Soglia, J. R.; Zhao, S. X. Can In Vitro Metabolism-Dependent Covalent Binding Data in Liver Microsomes Distinguish Hepatotoxic from Nonhepatotoxic Drugs? An Analysis of 18 Drugs with Consideration of Intrinsic Clearance and Daily Dose. *Chem. Res. Toxicol*. 2008, *21*, 1814-1822.

(38) Orhan, H.; Vermeulen, N. P. E. Conventional and Novel Approaches in Generating and Characterization of Reactive Intermediates from Drugs/Drug Candidates. *Curr. Drug Metab.* 2011, *12*, 383-394.

(39) Baillie, T. A. Metabolism and Toxicity of Drugs. Two Decades of Progress in Industrial Drug Metabolism. *Chem. Res. Toxicol*. 2008, *21*, 129-137.

(40) WO2005016894 and WO2004080980

(41) Strazzolini, P.; Giumanini, A. G., Runcio. A. Nitric acid in dichloromethane solution. Facile preparation from potassium nitrate and sulfuric acid. *Tetrahedron Lett.* 2001*, 42(7)*, 1387-1389.

(42)**.** Bossi, R.T., Saccardo, M.B., Ardini, E., Menichincheri, M., Rusconi, L., Magnaghi, P., Orsini, P., Avanzi, N., Borgia, A.L., Nesi, M., Bandiera, T., Fogliatto, G., Bertrand, J.A. Crystal structures of anaplastic lymphoma kinase in complex with ATP competitive inhibitors. Journal: (2010) Biochemistry 49: 6813-6825.

(43) Richmond, W.; Wogan, M.; Isbell, J.; Gordon, W. P. Interstrain differences of in vitro metabolic stability and impact on early drug discovery. *J. Pharm. Sci.* 2010, *99*, 4463-4468.

(44) www.clinicaltrials.gov (NCT01283516; NCT01634763; NCT01685060; NCT01685138; NCT01772797; NCT01742286; NCT01828099; NCT01828112)

(45) Shaw, A. T.; Camidge, D. R.; Felip, E.; Sharma, S.; Tan, D. S. W.; Kim, D.; De Pas, T.; Vansteenkiste, J. F.; Santoro, A.; Liu, G.; Goldwasser, M.; Dai, D.; Boral, A. L; Mehra, R.

Results of a First-in-Human Phase I Study of the ALK Inhibitor LDK378 in Advanced Solid Tumors. *Ann Oncol*. 2012, *23 (suppl 9),* ix153.

(46) Yuan, D.; Uvarova, V.; Isbell J. Peak Seeker: An Algorithm for Rapid Determination of Solubility. *J. Laboratory Automation*. 2005, *10*, 254-257.

(47) Bell, L.; Bickford, S.; Nguyen, P. H.; Wang, J.; He, T.; Zhang, B.; Friche, Y.; Zimmerlin, A.; Urban, L.; Bojanic, D. Evaluation of Fluorescence- and Mass Spectrometry—Based CYP Inhibition Assays for Use in Drug Discovery. *J. Biomol. Screen.* 2008, *13*, 343-353.

(48) Matthews D. R.; Hosker J. P.; Rudenski A.S.; Naylor B.A.; Treacher D.F.; Turner R.C. Homeostasis model assessment: insulin resistance and β-cell function from fasting plasma glucose and insulin concentrations in man. *Diabetologia* 1985, *28*, 412–419.

TOC